

# Triadic analysis of affiliation networks

JASON CORY BRUNSON

Center for Quantitative Medicine, UConn Health, Farmington, CT 06030

(e-mail: brunson@uchc.edu)

---

## Abstract

The widely-used notion of triadic closure has been conceptualized and measured in a variety of ways, most famously the clustering coefficient. This paper proposes a measure of triadic closure in affiliation networks designed to control for the influence of bicliques. In order to avoid arbitrariness, the paper introduces a triadic framework for affiliation networks, within which a range of possible statistics can be considered; it then takes an axiomatic approach to narrowing this range. The paper conducts an instrumental assessment of the proposed statistic alongside two previous proposals, for reliability, validity, and usefulness. Finally, these tools demonstrate their collective applicability in a multi-perspective investigation into triadic closure in several empirical social networks.

---

## 1 Introduction

Triadic analysis, which emphasizes the interactions within subsets of three nodes, has long been central to network science, including the development of popular diagnostics and random null models and their application to empirical data. Meanwhile, affiliation (or co-occurrence) data have long been a major source of empirical networks, and a range of diagnostics and models have been tailored to their higher-order structure. However, no actor-centric triadic analyses of affiliation networks are known to the author. This paper describes such a study, motivated by the need for a new measure of triadic closure.

### 1.1 Background

**Precursors** Two threads from the network literature illustrate the triad-centric perspective pursued in Sec. 2 and provide background for the hypotheses and tests of Sec. 3.

1. Cognitive balance theory can be understood to make predictions about the social relations among triads of individuals, and a series of early social network studies pursued this line of inquiry (Davis, 1967). Graph-theoretically, different constraints on a network's triads imply different organizational structures for the aggregate network, with different sociological interpretations. The triad-level predictions, and therefore their socio-structural implications, could then be tested against the triad censuses of empirical networks. A simple example was transitivity, the principle that the (directed) relations  $p \rightarrow q \rightarrow r$  imply the relation  $p \rightarrow r$ . Taken as an axiom, this produced the transitive graph model, which has a hierarchical global structure characterized by “ranked clusters” (Holland & Leinhardt, 1971). Research on transitive graphs led to the transitivity ratio, which measures how nearly transitive a directed graph is (Harary & Komrel, 1979).

2. Empirical social networks tend to exhibit the “small world” property, a high concentration of ties within communities yet counterintuitively low distances between actors in different communities (de Sola Pool & Kochen, 1978). The “strong triadic closure” (STC) hypothesis proposed to reconcile these properties by ascribing a cohesion role to strong ties within communities and a bridging role to weak ties between them (Granovetter, 1973). STC distinguishes two levels of tie (strong and weak) and posits that strong ties lead to more TC. The “structural holes” framework reoriented this picture to focus on the neighborhood of one actor. In this framework, an actor with many weak ties sees a shortage of relations among their neighbors provide opportunities for brokerage (Burt, 1992). This work introduced constraint, a measure of local TC as it constrains such opportunities. A later (unrelated) study introduced a simpler actor-level measure of TC called the clustering coefficient in order to compare “cliquishness” across a family of small world models (Watts & Strogatz, 1998).

**Conventions** The present study concerns social networks, though the concepts generalize to any affiliation network setting. Most of the terminology and notation used here is taken from standard references for graph theory (Bondy & Murty, 2008) and social network analysis (Wasserman & Faust, 1994). Additional concepts will be defined as needed.

A graph  $G = (V, E)$  consists of a finite set  $V$  of nodes and a set  $E \subseteq V \times V$  of edges  $e = (v, w)$ . Edges will be symmetric and will not include duplicates or loops. A graph is bipartite if its nodes can be partitioned into subsets  $V_1$  and  $V_2$  in such a way that  $E \subseteq V_1 \times V_2$ . The degree of a node  $v$  is the number of edges containing  $v$ . A subgraph of  $G$  is a graph  $G' = (V', E')$  satisfying  $V' \subseteq V$  and  $E' \subseteq E$ , and a subset  $W \subseteq V$  of nodes induces the subgraph  $(W, E \cap (W \times W))$ .

Traditional social networks consist of actors having relations among them, and are modeled as graphs with actors represented by nodes and relations by edges. (For present purposes, relations are symmetric.) Three actors, together with the relations among them, form a triad; *triadic closure* (TC) refers to the tendency for the relations  $(p, q)$  and  $(q, r)$  to entail the relation  $(p, r)$  (see Fig. 1a,b). The triads of a traditional network  $G$  take four types  $i = 0, 1, 2, 3$ , according as the actors have zero, one, two, or three relations among them; the tallies  $s_i = s_i(G)$  of each type constitute the *triad census*  $(s_0, s_1, s_2, s_3)$ . The *(classical) clustering coefficient*, a measure of TC often described as the proportion of connected triples that are closed (Newman, 2003), can then be expressed as the ratio  $C(G) = 3 \times s_3 / (s_2 + 3 \times s_3)$ .

Relations among the actors of an *affiliation network* (AN) are established through common attendance at events; each event is attended by some subset of actors. ANs are modeled as bipartite graphs,  $V_1$  consisting of the actors and  $V_2$  the events. Though actors are only tied to events, in both settings the neighbors of an actor  $v$  shall be the actors related to  $v$ . If pairs of actors are assigned edges according as they coattended events, then they form a traditional social network called the projection (see Figs. 2 and 4). If the relations of a traditional network, or the events of an AN, occur at specific moments in time, then call the network dynamic (otherwise, static).

**Organization** Sec. 1.2 presents the proposed clustering coefficient. The main body of the paper is split between theoretical (Sec. 2) and empirical (Sec. 3) evaluations of this statistic,

both of which begin with their own organizational outline. In short, Sec. 2 explores triadic analysis in the abstract, while Sec. 3 compares triadic analyses on empirical data. Sec. 4 summarizes the paper, identifies limitations of the study, and suggests directions for future work.

All analyses are performed, and all images produced, using the open-source statistical programming language R, with the `igraph` and `ggplot2` packages in particular (R Development Core Team, 2008; Csardi & Nepusz, 2006; Wickham, 2009). Code to reproduce all analyses is available at <https://github.com/corybrunson/triadic>.

### 1.2 The exclusive clustering coefficient

**Motivation** This study was motivated by the need for a measure of TC in ANs that controls for the influence of (often recurring) events among several actors. The popular clustering coefficient  $C$  is applied to ANs by way of their projection to traditional networks; this shall be the meaning of the shorthand  $C(G)$ .<sup>1</sup> Though  $C$  is actor-centric, in that events do not play directly into its calculation, the proliferation of 3-edge triads due to high-attendance events often dominates its behavior (Newman, 2001; Glänsel & Schubert, 2004). This has several consequences for its use: First, its values are concentrated at the upper end of the theoretical range  $[0, 1]$ , rendering any single value of  $C$  less informative (see Sec. 3.1). Second, the value of  $C$  is largely determined by event sizes, rather than by more intricate interactions among actors (Newman *et al.*, 2001). Third, for this reason  $C$  is a poor indicator of *dynamic* TC in ANs (see later this section), contrary to its (reasonable) sometimes interpretation (Martin *et al.*, 2013).

Previous attempts to identify and quantify other sources of TC in ANs have taken both “conversion” and “direct” approaches (Borgatti & Halgin, 2011). Conversion approaches have, for example, standardized the value of  $C$  by its values at an equivalent null model (Uzzi & Spiro, 2005) or applied clustering coefficients designed for weighted networks to weighted projections of ANs (Saramäki *et al.*, 2007). These approaches have successfully discriminated among otherwise similar ANs but provide limited insight into underlying processes. Two recent direct approaches introduced clustering coefficients that incorporate AN structure into their calculation (Opsahl, 2013; Liebig & Rao, 2014). The stark differences in their designs was inspirational to the approach in Sec. 2.3.

**Design** Perhaps the most conspicuous difference in practice between social networks constructed directly from relational data versus implicitly from affiliation data is the proliferation of cliques in the latter, due to events attended by several actors. The clique graph  $K_n$  consists of  $n$  nodes and all  $\binom{n}{2}$  possible edges among them; any  $n$  actors who attend some common event in an AN constitute a copy of  $K_n$  in its projection. This introduces  $\binom{n}{3}$  3-edge triads. Taken over all events, these can dramatically increase  $C(G)$  when  $G$  is an AN (see Ex. 2.3). This arises from the comparison of null models: Sampling from the possible bipartite graphs having the same actor and event degrees as  $G$  yields projections with much higher clustering coefficients than sampling from the possible graphs having the same actor degrees as the projection of  $G$  (Newman *et al.*, 2001).

<sup>1</sup>  $C$  evaluates to zero on any bipartite graph.

One direct attempt to control for the influence of high-attendance events requires that “connected triples” form only when distinct events connect different pairs of actors. This inspired the *Opsahl clustering coefficient  $C^*$* , defined as the proportion of 4-paths that are closed: The graph  $P_d$  consisting of distinct nodes  $v_0, v_1, \dots, v_d$  and edges  $(v_i, v_{i+1})$  is called the  $d$ -path; if, instead,  $v_0 = v_d$ , the result is the  $d$ -cycle  $C_d$ .<sup>2</sup> (Both have  $d$  edges; see Fig. 1c,d.) For a 4-path in  $G$  to be “closed” means for it to be contained in a 6-cycle.<sup>3</sup> Propitiously, in an empirical test,  $C^*$  took much smaller values than  $C$ , and the two statistics diverged most on the network with the greatest mean event size (Opsahl, 2013).

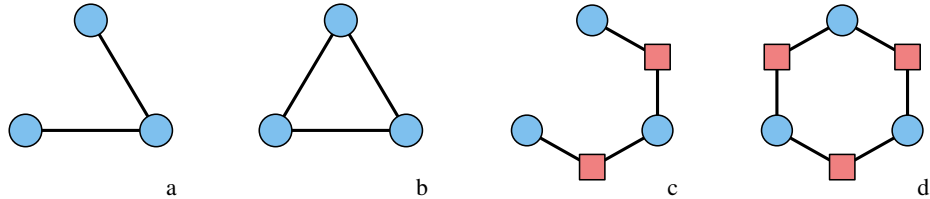


Fig. 1: Traditional and affiliation network conceptions of triadic closure: In traditional networks, the 2-edge triad (a) is “open” while the 3-edge triad (b) is “closed”. The clustering coefficient  $C$  is defined either as a ratio of the numbers of triads of these types (see Sec. 1.1) or as the proportion of subgraphs of the form (a) that are contained in a subgraph of the form (b). One extension of this idea to ANs uses the 4-path (c) and the 6-cycle (d) in place of these triads. The Opsahl clustering coefficient  $C^*$  is defined as the proportion of subgraphs (c) that are contained in a subgraph (d). (Circular nodes denote actors; square nodes denote events.)

However, just as  $C$  is sensitive to cliques,  $C^*$  is sensitive to bicliques: The biclique graph  $K_{n,m}$  consists of  $n$  actors,  $m$  events, and all  $n \times m$  possible actor–event edges—so that, for example, if  $m \geq 3$ , then the biclique  $K_{3,m}$  contains  $6 \times m(m-1)$  4-paths, each of which is closed.<sup>4</sup> The effect grows geometrically as  $n$  increases. Thus the value of  $C^*$  may be dominated by influences that produce bicliques—specifically, repeat coattendance, the same subset of actors attending more events than expected by chance. This is a plausible outcome of social dynamics and has been observed in empirical networks (Carrino, 2006).

$C^*$  introduces another consideration: What population is being surveyed, from which the clustering coefficient is calculated? In the case of  $C$ , the answer could be triads, as in the definition above; or it could be 2-paths as in the popular definition (Newman, 2003). In the case of  $C^*$ , the answer is 4-paths, which are motifs involving both actors and events. Depending on the context, it may be preferable to survey such actor–event motifs or subsets of actors alone (as in the case of  $C$ ). Sec. 2.3 considers this choice in detail; for now, it is enough that the triad-centric perspective favors weighting all triads—hence, all actors—equally.

<sup>2</sup> The 4-paths involved in this calculation must begin and end at actor nodes.

<sup>3</sup> Several other studies have proposed bipartite clustering coefficients that do not concern triples of actors, so are not considered here (Opsahl, 2013).

<sup>4</sup> Though note that  $K_{3,2}$  contains  $6 \times 2 = 12$  open 4-paths.

The proposed statistic addresses these concerns in two ways: First, the 4-paths and 6-cycles in the calculation should contain no intermediate edges; i.e., each event should be attended only by two of the three actors. This mitigates the influence of bicliques. Second, any ordered triple of actors counts at most once, either open or closed. This has the effect (see Thm. 2.7) of weighting triads equally. The result is a statistic denoted  $C^\circ$ . In everyday language,  $C^\circ$  asks, *provided  $p$  and  $q$  attend some event without  $r$ , and  $q$  and  $r$  attend some event without  $p$ , what is the probability that  $p$  and  $r$  attend some event without  $q$ ?* Since  $C^\circ$  measures TC only through pairwise-exclusive events, it shall be called the *exclusive clustering coefficient*.

*Example 1.1*

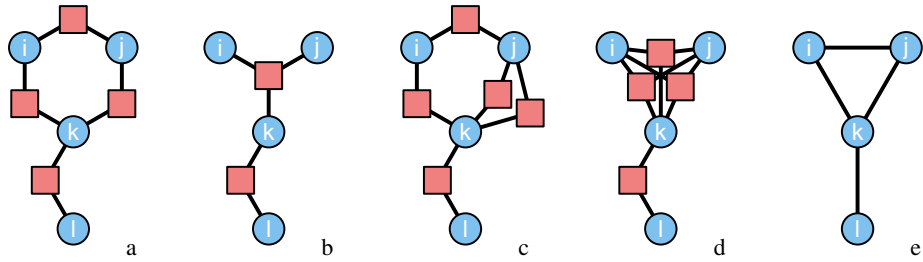


Fig. 2: Four ANs (a-d) having the same projection (e).

Fig. 2 depicts four ANs that project to the same the “kite” graph. A comparison of (a) and (b) illustrates the shared objective of  $C^*$  and  $C^\circ$ : (a) exhibits TC in the sense of interest, while (b) is TC of the kind  $C^*$  was designed to ignore. Both  $C^*$  and  $C^\circ$  take the same global ( $\frac{3}{5}$ ) and local (see Def. 2.4) values as  $C$  on (a), but are uniformly zero on (b). ANs (c) and (d), however, illustrate differences between  $C^*$  and  $C^\circ$ :  $C^*$  evaluates globally to  $\frac{5}{8}$  on (c) and to  $\frac{3}{4}$  on (d), due to different numbers of copies of  $P_4$  and  $C_6$ . For instance, six copies of  $P_4$  in (d) proceed from  $i$  through  $j$  to  $k$ , and each is closed.  $C^\circ$ , in contrast, takes the same values on (c) and (d) as on (a) and (b), respectively—indeed, the same number of open and closed 4-paths appear in the calculation.

By eliminating other sources of 3-edge triads,  $C^\circ$  may also prove useful in gleaning dynamic information from a static snapshot. In the dynamic setting, TC often refers to the tendency for actors who are not neighbors, but who have neighbors in common at one time, to *become* neighbors at a later time (David & Jon, 2010; Martin *et al.*, 2013). Here, the *dynamic triadic closure*  $D(G)$  of a dynamic network  $G$  shall be, among those triads at which there is at some time an open 2-path, the proportion at which there is at a later time a 3-cycle. If  $G$  is an AN, then  $D$ , like  $C$ , is calculated on its projection. In the traditional setting, if a dynamic network has no simultaneous edges, then  $D = s_3/(s_2 + s_3) = C/(3 - 2 \times C)$ . In the AN setting, pairwise-exclusive events are essential to  $D$ , since an open 2-path in the projection must correspond to a triad with only pairwise-exclusive events. While other factors introduce disagreements (existence of earlier events shared by each member of a triad; such an event, rather than a third pairwise-exclusive event, “closing” an open 2-path), it stands to reason that  $C^\circ$  may provide a useful estimate of  $D$ .

## 2 Theoretical analyses

This section formalizes the exclusive clustering coefficient and evaluates its theoretical merits. Sec. 2.1 develops a formal notion of “triad” for ANs. On this foundation, Sec. 2.2 unifies  $C$ ,  $C^*$ , and  $C^\circ$  into a generic clustering coefficient. This definition specializes to impractically many statistics, which Sec. 2.3 whittles down by appeal to several qualities suited to present purposes. The technical details of this process are relegated to Sec. 2.4.

### 2.1 Triads

**Scheduled subgraphs** What is a “triad”? A triad-centric approach to ANs requires, first, an object of study. Since the triads of a traditional network are the subgraphs *induced* by three actors,<sup>5</sup> a suitable analog of induced subgraphs for ANs would provide an analogous notion of triad. Accordingly, this paper proposes that those events be included that establish relations among a set of actors:

#### Definition 2.1

Given an AN  $G$  and a subset  $W$  of actors of  $G$ , the subgraph of  $G$  *scheduled* by  $W$  is the subgraph induced by the actors  $W$  together with all events attended by at least two actors in  $W$ . *Scheduled* graph maps are defined analogously to induced graph maps, and the *triads* of  $G$  are the subgraphs scheduled by three actors.

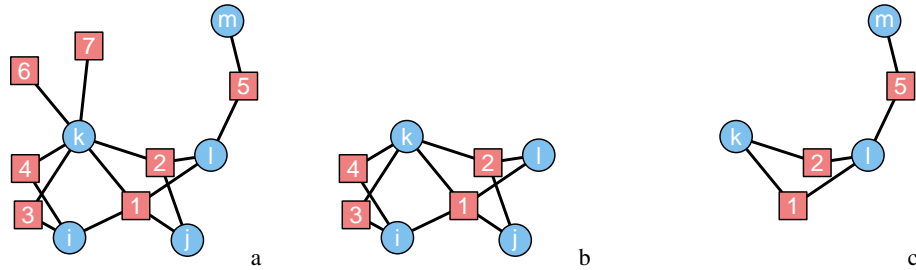


Fig. 3: An AN (a) of actors  $i, j, k, l, m$  and its scheduled subgraphs (b) at  $\{i, j, k, l\}$  and (c) at  $\{k, l, m\}$ .

#### Example 2.2

Fig. 3 depicts an AN of five actors and two of its scheduled subgraphs. Note in particular that the scheduled subgraph on the entire set of actors (not shown) does not include the events labeled 6 and 7, since they play no role in establishing relations among the actors.<sup>6</sup>

<sup>5</sup> Notably, this notion has been extended to multiplex networks, which have one type of node but multiple types of edges (Cozzo *et al.*, 2013).

<sup>6</sup> This shows that an AN need not be the scheduled subgraph of its actors, contrary to the analogous property of induced subgraphs. Their projections, however, are the same (up to edge weights).

**Triad censuses** The classification of AN triads is straightforward but not trivial. While traditional triads fall into four isomorphism classes, AN triads, in theory, occupy arbitrarily many, due to the unlimited number of events two or three actors might attend. Consider an arbitrary triad with actors  $p, q, r$ . Take  $w_{pq}$  to be the number of events attended by  $p$  and  $q$ , similarly define  $w_{qr}$  and  $w_{pr}$ , and take  $w_{pqr}$  to be the number of events attended by all three. (Note that  $w_{pq}$  does not depend on  $r$ , etc.) Up to isomorphism, it may be assumed that  $w_{pq} \geq w_{qr} \geq w_{pr}$  (otherwise just rename the actors). Necessarily,  $w_{pqr} \geq w_{pq}$ .<sup>7</sup> Let  $\mu = (\mu_1, \mu_2, \mu_3) = (w_{pq} - w_{pqr}, w_{qr} - w_{pqr}, w_{pr} - w_{pqr})$  count the “exclusive” events between each pair of actors, and let  $w = w_{pqr}$  count the “inclusive” events attended by all three. The pair  $(\mu, w)$  determines the isomorphism class of the triad. Since  $\mu_1 \geq \mu_2 \geq \mu_3$ ,  $\mu$  is an integer partition of three parts; write  $\mu \in \text{Par}_3$ . Where  $\mathbb{Z}_{\geq 0}$  is the set of nonnegative integers and  $\mathcal{T}$  is the set of triad isomorphism classes, this gives a bijective correspondence

$$\mathcal{T} \leftrightarrow \text{Par}_3 \times \mathbb{Z}_{\geq 0}.$$

Write  $\text{Tr}_{\mu w}$  for the triad described above, and  $s_{\mu w} = s_{\mu w}(G)$  for the number of triads of  $G$  isomorphic to  $\text{Tr}_{\mu w}$ . The (*full*) *triad census* of  $G$  is then the array  $(s_{\mu w})_{\mu, w}$ . The partitions  $\text{Par}_3$  can be totally ordered, and thereby the census arranged in a matrix, whose size depends on the network.<sup>8</sup> Necessarily,  $\sum_{\mu, w} s_{\mu w} = \binom{|V_1|}{3}$ . The triads scheduled from  $i, j, k$  in Fig. 2 (a–d), for example, are  $\text{Tr}_{(0,0,0),1}$ ,  $\text{Tr}_{(1,1,1),0}$ ,  $\text{Tr}_{(2,1,1),0}$ , and  $\text{Tr}_{(2,1,1),0}$ .

This scheme explodes as networks grow dense. The following alternative scheme is instead bounded, but nonetheless captures useful affiliation structure: The events of a triad fall into four structural equivalence classes, according to which actors attend them. Instead of binning triads by *how many* events they have in each class, bin them by whether they contain *some* event in each class. If  $\text{Tr}_{\mu w}$  has, for example, any inclusive event (i.e., if  $w > 0$ ), then  $\text{Tr}_{\mu w}$  shares a bin with  $\text{Tr}_{\mu,1}$ ; otherwise it is  $\text{Tr}_{\mu,0}$ . Each bin then contains exactly one representative  $\text{Tr}_{\mu w}$  with  $\mu_1, \mu_2, \mu_3, w \in \{0, 1\}$ , and this bin is determined by the two numbers  $x = \mu_1 + \mu_2 + \mu_3$  and  $y = w$ . The *structural triad census* consists of the eight tallies  $t_{xy}$  of triads in each bin, taken over  $0 \leq x \leq 3$  and  $0 \leq y \leq 1$ . Though in practice containing only twice as many as the simple census, the structural census contains useful additional information (see Thm. 2.7 and Sec. 3.1).

### Example 2.3

The network DDGGS2, depicted in Fig. 4 with its full census and its projection, is taken from a famous study of the American caste system (Davis *et al.*, 1941). As an example of a unit of social analysis, the study presented attendance data for five acquainted women (“Miss A” through “Miss E”) and five social activities (bridge, dinner, movies, dance, and visiting), forming an AN. The projection contains three 2-edge and seven 3-edge triads, so the simple census is  $(0, 0, 3, 7)$ . (Therefore, incidentally,  $C(\text{DDGGS2}) = \frac{3 \times 7}{3+3 \times 7} = \frac{7}{8}$ .)

<sup>7</sup> A storage-friendly enumeration of the triad classes is given by the quadruple of nonnegative integers  $w_{pqr} - w_{pq}, w_{pq} - w_{qr}, w_{qr} - w_{pr}, w_{pr}$ . A more intuitive scheme is used in the text.

<sup>8</sup> Where  $n = \max(\mu)$ , there are bijections  $\sigma : \text{Par}_3^{(n)} \rightarrow \{\binom{n+3}{3}\}$ , from the partitions in  $\text{Par}_3$  having parts  $\leq n$  to the subsets of  $\{1, \dots, n+3\}$  of size 3, and  $\rho : \{\binom{n+3}{3}\} \rightarrow \{1, \dots, \binom{n+3}{3}\}$ , which indexes these subsets; their composition  $\rho \circ \sigma : \text{Par}_3^{(n)} \rightarrow \{1, \dots, \binom{n+3}{3}\}$  indexes the partitions.  $\sigma$  is a classical bijection (Stanley, 2002);  $\rho$  is the *revolving door ordering* of  $\{\binom{n+3}{3}\}$  (Kreher & Stinson, 1999).

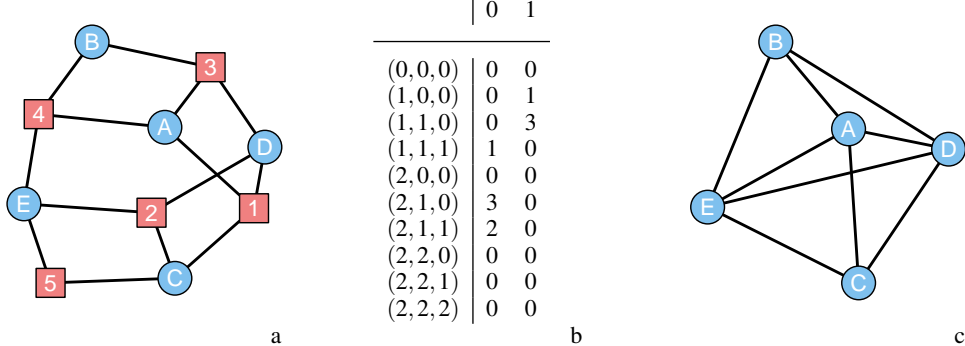


Fig. 4: The network DDGG2 (a), its full triad census (b), and its projection (c). The column in (b) indicates the number of inclusive events; the row indicates the distribution of exclusive events across pairs of actors. For example, the triad at (A, B, C) is tallied in column 0, row (2, 1, 0) (see Ex. 2.3).

These tallies, however, obscure the affiliation structure: The seven fully-connected triads fall into four triad classes. One might be called both “symmetric” and “exclusive”: Ms. B, D, and E attended no events together, but each pair were present at one, so that their triad is (isomorphic to)  $\text{Tr}_{(1,1,1),0}$ . Two triads were similarly exclusive but not symmetric: Ms. C and E attended two events without Ms. A, though Ms. A attended different, separate events with Ms. C and E; they thus form a triad  $\text{Tr}_{(2,1,1),0}$ , as do Ms. A, D, and E. The remaining four might be called “inclusive”, in that all three women attended some event together (specifically, the four activities of attendance 3). In each case, at least one pair of women attended another event together, forming the triads  $\text{Tr}_{(1,0,0),1}$  and  $\text{Tr}_{(1,1,0),1}$ . The women constituting each of the three 2-edge triads joined in no single activity together, instead forming four copies of  $\text{Tr}_{(2,1,0),0}$ . For example, Ms. A and B attended two events together, Ms. A and C one, and Ms. B and C none. (See also Table 2.)

## 2.2 Category framework

**Graph maps** The generic clustering coefficient will be defined in terms of graph maps. For present purposes, a graph map  $\phi : G \rightarrow H$  “from  $G$  to  $H$ ” shall assign each node  $v$  of  $G$  to a node  $\phi(v)$  in  $H$  (the image of  $v$  under  $\phi$ ) in such a way that every edge  $(v, w)$  in  $G$  is preserved, in that  $(\phi(v), \phi(w))$  is an edge in  $H$ . One example is the inclusion of a subgraph  $G \subseteq H$ . A graph map  $\phi : G \rightarrow H$  is called induced if the image  $\phi(G) \subseteq H$  is an induced subgraph. The images  $\phi(v)$  in  $H$  and the preserved edges among them form the image of  $G$  in  $H$ . Two graph maps  $\phi : G \rightarrow H$  and  $\psi : H \rightarrow K$  yield the composition  $\psi \circ \phi : G \rightarrow K$  defined by  $\psi \circ \phi(v) = \psi(\phi(v))$ . Such a graph map  $\psi \circ \phi : G \rightarrow K$  is said to factor through  $H$ ; for example, any map  $\phi : G \rightarrow H$  factors through its image  $\phi(G) \subseteq H$ .

A graph map  $\phi : G \rightarrow H$  is injective if it sends no two nodes in  $G$  to the same node in  $H$ , and surjective if every node in  $H$  is the image of some node in  $G$  (its pre-image); by a “copy” of  $G$  in  $H$ , or a path or cycle “in  $G$ ”, is, technically, meant the image of such an injective map. (By convention, paths and cycles in an AN arise from maps that send  $v_0$  to an actor. Thus a 4-path  $\phi : P_4 \rightarrow G$  is closed if it factors through  $C_6$ .

An injective, surjective map is bijective, and a bijective map  $\phi : G \rightarrow H$  is an isomorphism if it is induced—that is, if it preserves absences of edges  $((\phi(v), \phi(w)) \notin G \text{ whenever } (v, w) \notin H)$ . The isomorphisms establish an equivalence relation on graphs, so that two graphs related by an isomorphism are said to be isomorphic, and to lie in the same isomorphism class. Two nodes  $v, w \in G$  are structurally equivalent if there is an isomorphism  $G \rightarrow G$  that sends every node to itself except exchanges  $v$  and  $w$ ; this establishes an equivalence relation on the nodes of  $G$ .

**Categories** While not strictly necessary, the framework of category theory absorbs several useful and unobjectionable yet messy assumptions into the notation, provides a catalogue of natural examples, and avoids introducing hidden constraints on the range of possibilities.<sup>9</sup>

A category  $\mathcal{C}$  consists of a set of objects; for each pair of objects  $(A, B)$ , a set  $\text{Hom}_{\mathcal{C}}(A, B)$  of morphisms from  $A$  to  $B$ ; and, for each pair of morphisms  $f \in \text{Hom}_{\mathcal{C}}(B, C)$  and  $g \in \text{Hom}_{\mathcal{C}}(A, B)$ , the composition  $f \circ g \in \text{Hom}_{\mathcal{C}}(A, C)$ ; all subject to the following conditions (Mitchell, 1965):

- i. (Identity) For every  $A \in \mathcal{C}$  there exists  $\text{id}_A \in \text{Hom}_{\mathcal{C}}(A, A)$  satisfying  $f \circ \text{id}_A = f$  and  $\text{id}_A \circ g = g$  for any  $f \in \text{Hom}_{\mathcal{C}}(A, B)$  or  $g \in \text{Hom}_{\mathcal{C}}(C, A)$ .
- ii. (Associativity) For any triple of morphisms  $f \in \text{Hom}_{\mathcal{C}}(C, D)$ ,  $g \in \text{Hom}_{\mathcal{C}}(B, C)$ , and  $h \in \text{Hom}_{\mathcal{C}}(A, B)$ ,  $f \circ (g \circ h) = (f \circ g) \circ h$ .

A subcategory  $\mathcal{C}' \subseteq \mathcal{C}$  consists of the same objects as  $\mathcal{C}$  and subsets  $\text{Hom}_{\mathcal{C}'}(A, B) \subseteq \text{Hom}_{\mathcal{C}}(A, B)$  that also form a category. A congruence relation  $\sim$  on  $\mathcal{C}$  consists of equivalence relations  $\sim_{A, B}$  on each  $\text{Hom}_{\mathcal{C}}(A, B)$  that are compatible with the composition of morphisms, so that the quotient category  $\mathcal{C} / \sim$  is determined by the objects of  $\mathcal{C}$  and the equivalence classes of morphisms of  $\mathcal{C}$  under  $\sim$ .

Henceforth, view  $\mathcal{T}$  as the category of AN triads, with morphisms the graph maps  $\phi : H \rightarrow K$  between triads that assign the actors of  $H$  to distinct actors of  $K$  (therefore sending events only to events), and with composition given by  $(f \circ g)(v) = f(g(v))$ .  $\mathcal{T}$  can be viewed as a subcategory of the category of graphs (Hell, 1979). Write  $\text{Hom}_{\mathcal{T}}^K(G, H)$  for the set of morphisms from  $G$  to  $H$  that factor through  $K$ . If  $G$  is any AN, write  $\text{Hom}_{\mathcal{T}}(H, G)$  for the set of all morphisms from the triad  $H$  to any triad of  $G$ .

**Clustering coefficients** The three clustering coefficients described in Sec. 1.2 can now be expressed in category-theoretic terms. Let  $\approx$  denote the congruence relation on  $\mathcal{T}$  given by taking any two maps that agree on actors to be congruent. For example, there is only one

<sup>9</sup> Why categories? While AN triads are innumerable, their combinatorial complexity is nonetheless limited (see Sec. 2.1). It would be short work to classify a substantial subset (19, by the author's count) of clustering coefficients (in the sense of Def. 2.4), including  $C$ ,  $C^*$ , and  $C^o$ , according to which structural equivalence classes of events (exclusive, distinct inclusive, or same inclusive) the events of  $W$  and  $X$  may be mapped to, and which of these should then be considered congruent. This scheme, however, would omit more ad hoc clustering coefficients, for instance one that requires the events  $v_1, v_3$  of  $W$  to be mapped to exclusive events but places no such constraint on  $v_5$  in  $X$ . Such a statistic would violate Axiom 1, but may be very useful in certain settings or to address certain problems (compare to the discussion of STC in Sec. 3.2). The category-theoretic framework remains abstract enough to avoid these omissions.

graph map from  $P_4$  to the kite graph (a) in Fig. 2 that sends  $v_0, v_2, v_4$  to  $i, j, k$  (respectively), and likewise only one such map to (b). However, there are several such maps to (c), which are all congruent in  $\mathcal{T}/\approx$ . It turns out that, for an affiliation network  $G$ ,

$$C(G) = \frac{|\text{Hom}_{\mathcal{T}/\approx}^{C_6}(P_4, G)|}{|\text{Hom}_{\mathcal{T}/\approx}(P_4, G)|} = \frac{|\text{Hom}_{\mathcal{T}/\approx}(C_6, G)|}{|\text{Hom}_{\mathcal{T}/\approx}(P_4, G)|}. \quad (1)$$

The previous proposal (Opsahl, 2013) restricted the morphisms in Eq. 1 to injective graph maps. It is straightforward to check that these form a subcategory  $\widetilde{\mathcal{T}} \subset \mathcal{T}$ . No congruence relation was imposed; for consistency of notation, one can write  $\widetilde{\mathcal{T}}/ =$  for  $\widetilde{\mathcal{T}}$ , where  $=$  denotes equality of graph maps.  $C^*$  is then realized as

$$C^*(G) = \frac{|\text{Hom}_{\widetilde{\mathcal{T}}/ =}^{C_6}(P_4, G)|}{|\text{Hom}_{\widetilde{\mathcal{T}}/ =}(P_4, G)|}, \quad (2)$$

analogously to the first formulation in Eq. 1. The present proposal further restricts the morphisms in Eq. 2 to induced injections. These turn out to form their own subcategory  $\overline{\mathcal{T}} \subset \widetilde{\mathcal{T}}$ . Additionally, the graph maps that agree on actors *and that send events to structurally equivalent images* constitute a congruence relation  $\simeq$  (on  $\overline{\mathcal{T}}$  or  $\mathcal{T}$ ), which is weaker than  $\approx$  in that the congruence classes of  $\approx$  are unions of those of  $\simeq$ . The statistic  $C^\circ$  can then be realized as

$$C^\circ(G) = \frac{|\text{Hom}_{\overline{\mathcal{T}}/\simeq}^{C_6}(P_4, G)|}{|\text{Hom}_{\overline{\mathcal{T}}/\simeq}(P_4, G)|} = \frac{|\text{Hom}_{\overline{\mathcal{T}}/\simeq}(C_6, G)|}{|\text{Hom}_{\overline{\mathcal{T}}/\simeq}(P_4, G)|}. \quad (3)$$

### 2.3 Axiomatic approach

**General formulation** What is a “clustering coefficient” (in the AN context)? Sec. 2.2 exhibited three variations on the idea. The goal of this section is to synthesize these variations into a single generic definition.

The statistics  $C$  and  $C^*$  differ in three respects: the choice between the formulations in Eq. 1 (which need not agree), the subcategory of graph maps from which the morphisms in Eq. 1 are drawn, and the congruence relation imposed on these morphisms. Whereas  $P_4$  (isomorphic to  $\text{Tr}_{(1,1,0),0}$ ) and  $C_6$  (isomorphic to  $\text{Tr}_{(1,1,1),0}$ ) are now recognizable as two among an infinite collection of distinct triads (see Fig. 5), a fourth choice is introduced: that of the “open” and “closed” ordered triple. Another direct approach (Liebig & Rao, 2014) considered three alternatives to  $C_6$ :  $\text{Tr}_{(1,1,0),1}$ ,  $\text{Tr}_{(1,0,0),2}$ , and  $\text{Tr}_{(0,0,0),3}$ . (These are the four AN triads whose duals are also triads, and in fact are self-dual (Breiger, 1974).) The corresponding alternatives to  $P_4$ , sometimes taken in pairs, were obtained by removing a single event from these. The following general formulation can be specialized with respect to each of these choices:

#### Definition 2.4

Pick canonical triads  $X \in \mathcal{T}$  and  $W \subset X$ , a subcategory  $\mathcal{C} \subseteq \mathcal{T}$ , and a congruence relation  $\sim$  on  $\mathcal{C}$ . A *(global) clustering coefficient* of  $G$  shall be a statistic of either form

$$\widehat{C}(G) = \frac{|\text{Hom}_{\mathcal{C}/\sim}^X(W, G)|}{|\text{Hom}_{\mathcal{C}/\sim}(W, G)|} \quad (\text{“rate of wedge closure”}) \text{ or} \quad (4)$$

$$\widehat{C}(G) = \frac{|\text{Hom}_{\mathcal{C}/\sim}(X, G)|}{|\text{Hom}_{\mathcal{C}/\sim}(W, G)|} \quad (\text{"alcove-to-wedge ratio"}), \quad (5)$$

where morphisms factor through  $X$  only by way of the subgraph relation  $\iota : W \rightarrow X$ . Call the morphisms  $\text{Hom}_{\mathcal{C}/\sim}(W, G)$  the *wedges* of  $G$ —closed if they factor through  $X$ , open if not—and  $\text{Hom}_{\mathcal{C}/\sim}(X, G)$  the *alcoves* of  $G$ .

Further designate a *center* actor  $v_c \in \{p, q, r\}$  in (each)  $W$ . Given an actor  $j \in G$ , obtain the (local) *clustering coefficient*  $\widehat{C}(j)$  of  $j$  by requiring of the morphisms in Eq. 4 or 5 that  $\phi(v_c) = j$  and  $\psi(\iota(v_c)) = j$ —that is, that wedges and alcoves are *centered* at  $j$ . The *wedge-dependent clustering coefficient*  $\widehat{C}_\ell$  of an affiliation network  $G$  shall be the mean value of  $\widehat{C}(j)$  across the actors  $j$  at which exactly  $\ell$  wedges are centered.

By letting  $X$  range over the four self-dual triads;  $\mathcal{C}$  over  $\mathcal{T} \supseteq \widetilde{\mathcal{T}} \supseteq \overline{\mathcal{T}}$ ;  $\sim$  over  $=, \simeq$ , and  $\approx$ ; and adopting either Eq. 4 or 5, Def. 2.4 specializes to  $4 \times 3 \times 3 \times 2 = 72$  distinct and fairly straightforward statistics, including  $C$ ,  $C^*$ , and  $C^\circ$ .<sup>10</sup> For present purposes, the best choice of  $X$  is clearly  $\text{Tr}_{(1,1,1),0}$ , leaving  $W = \text{Tr}_{(1,1,0),0}$ . These choices are assumed henceforth. (Note, however, that Thm. 2.6 does not require this assumption.)

Table 1: Three measures of global and local triadic closure in DDGGS2.

	Classical	Opsahl	Exclusive
DDGGS2	0.875	0.611	0.600
Miss A	0.833	0.500	0.500
Miss B	1.000	0.667	1.000
Miss C	1.000	0.667	0.500
Miss D	0.833	0.600	0.500
Miss E	0.833	0.714	0.750

### Example 2.5

Evaluations of  $C$ ,  $C^*$ , and  $C^\circ$  at DDGGS2 (Table 1) provide a compact comparison: One can tell from the local evaluations that the women occupy structurally distinct neighborhoods, though none of the statistics distinguishes them all. While  $C^*$  and  $C^\circ$  take lower values than  $C$ , the rankings of the actors are loosely correlated. Of particular interest are Miss B and C, whom  $C^*$  (and  $C$ ) do not distinguish but who take opposite values of  $C^\circ$ . At Miss B, the 4-path  $(A, 3, B, 4, E)$  is an open wedge to  $C^*$  but not a wedge at all to  $C^\circ$ ; at Miss C, the 4-path  $(D, 1, C, 5, E)$  is as a wedge to both  $C^*$  and  $C^\circ$  but only closed to  $C^*$ .

$C^*$  attributes high triadic closure to Miss C because her friends remain better connected when she is removed from the network, while the events she attended remain. In contrast,  $C^\circ$  attributes triadic closure to Miss B because her friends remain better connected when

<sup>10</sup> In fact, some of these turn out to be the same statistic; for example, assuming  $X = \text{Tr}_{(1,1,1),0}$ ,  $\mathcal{T}/\simeq$  and  $\overline{\mathcal{T}}/\approx$  both yield  $C^\circ$ .

she is removed from the network *along with the events she attended*. The statistic  $C^*$  thus detects triadic closure that relies in part on inclusive events, which  $C^\circ$  does not.<sup>11</sup>

The remainder of this section comes with a warning that the labeling schemes for triad nodes vary across contexts: Canonical triads  $\text{Tr}_{\mu w}$  have actors  $p, q, r$  such that  $w_{pq} \geq w_{qr} \geq w_{pr}$  (and unlabeled events);  $W$  and  $X$  adopt the schemes  $v_0, v_1, \dots$  for  $P_4$  and  $C_6$  from Sec. 1.2; and triads in target graphs of study are scheduled at (ordered) triples of actors  $(i, j, k)$  with events labeled with other lowercase roman letters.

**Axioms** As explained in Sec. 1.2, the main objective is to tailor  $\hat{C}$  to control for the influence of bicliques, and an auxiliary aim is for  $\hat{C}$  to weight actors equally. This section puts forth four properties  $\hat{C}$  might have. These should not be construed as necessarily desirable; they are motivated by the present objective. They also help organize the myriad statistics that arise from Def. 2.4 and provide easily verifiable criteria for them to satisfy stronger properties (Thms. 2.6, 2.7, and 2.8).

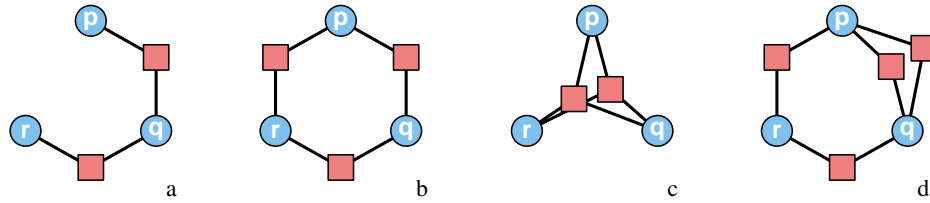


Fig. 5: Four AN triads from the axiomatic analysis: (a)  $\text{Tr}_{(1,1,0),0}$ , isomorphic to  $W$ ; (b)  $\text{Tr}_{(1,1,1),0}$ , isomorphic to  $X$ ; (c)  $\text{Tr}_{(0,0,0),2}$ , from the discussion of Axiom 4; and (d)  $\text{Tr}_{(2,1,1),0}$ , from the discussion of Lemma 2.14.

The first two axioms express two important features of  $C^*$ . In order to prevent single events from forming closed wedges,  $C^*$  is defined using only injections, from  $\mathcal{T}$ ; Axiom 1 requires that  $\mathcal{C}$  at least include induced injections. In order to allow distinct events to contribute distinct wedges,  $C^*$  removed the very strong congruence relation  $\approx$  imposed on the morphisms of  $C$ ; Axiom 2 forbids any two wedges or alcoves from being identified, whose events are not at least structurally equivalent.

#### *Axiom 1 (Induced injections)*

All induced injections (hence all isomorphisms) are morphisms (i.e.  $\mathcal{C}$  contains  $\mathcal{T}$ ).

#### *Axiom 2 (Structural equivalence)*

The images of an (event) node under congruent morphisms are structurally equivalent (i.e.  $\sim$  is no stronger than  $\simeq$ ).

The last two axioms address the goals of controlling for the influence of bicliques and of sampling over actors rather than motifs, identified in Sec. 1.2 (see Ex. 1.1). Axiom 3

<sup>11</sup> A stricter statistic might only recognize wedges and alcoves in triads who attend *no* common events (say, by restricting to scheduled maps in  $\mathcal{T}$ ), thereby measuring TC that is not accounted for, even redundantly, by coattendance by triads. This statistic would be  $3 \times t_{30} / (t_{20} + 3 \times t_{30})$ .

addresses the problem of sampling population by preventing several wedges from existing a single ordered triple. Axiom 4 addresses the influence of bicliques by attacking their symptom: the counterintuitive way that each actor of a triad can have a wedge with none of the wedges being closed, which is not possible under  $C$ . The idea is that two wedges with different centers “hook together” (overlap) at their shared “side” (pair of actors), closing each other, which is here called “wedge buckling”.  $C^*$  violates this idea, for example at Fig. 5c.

*Axiom 3 (Equal representation)*

At each ordered triple there exists exactly one of the following: no wedge, one open wedge, or one closed wedge.

*Axiom 4 (Wedge buckle)*

If wedges exist at two ordered triples with different centers in a triad, then both are closed.

**Theorems** Three useful properties follow from certain subsets of the axioms: two triadic formulations of  $\widehat{C}$ , which aide both conceptualization and computation, and one characterization. The proofs constitute the next section.

*Theorem 2.6 (Triad census formulation)*

For each triad  $\text{Tr}_{\mu w}$ , write the numbers

$$\begin{aligned} F_{\mu w} &= |\text{Hom}_{\mathcal{C}/\sim}(W, \text{Tr}_{\mu w}) \setminus \text{Hom}_{\mathcal{C}/\sim}^X(W, \text{Tr}_{\mu w})| \\ S_{\mu w} &= |\text{Hom}_{\mathcal{C}/\sim}^X(W, \text{Tr}_{\mu w})| \end{aligned}$$

of open and closed wedges, respectively, at  $\text{Tr}_{\mu w}$ . If  $\widehat{C}$  is defined using Eq. 4, then

$$\widehat{C}(G) = \frac{\sum_{\mu, w} s_{\mu w}(G) S_{\mu w}}{\sum_{\mu, w} s_{\mu w}(G) (F_{\mu w} + S_{\mu w})}. \quad (6)$$

Thm. 2.6 decomposes the rate-of-closure calculation into a ratio of motifs, according to the distribution of triads in  $G$ . The theorem proves useful in implementing the various global statistics, which may then be computed via arithmetic on the full census.

*Theorem 2.7 (Wedge binning formulation)*

Assume Axioms 1, 3, and 4. Then the triads of  $G$  can be binned into subsets  $S_\emptyset(G)$ ,  $S_W(G)$ , and  $S_X(G)$  according as they contain none, two open, or six closed wedges; and

$$\widehat{C}(G) = \frac{3|S_X(G)|}{|S_W(G)| + 3|S_X(G)|}. \quad (7)$$

Thm. 2.7 generalizes the description of  $C$  in Sec. 1 in terms of a smaller number of bins than the full census.  $C^*$  does not satisfy these criteria, though  $C$  and  $C^\circ$  do:  $C$  was defined in Sec. 1.1 via a specialization of this formula using the simple triad census, and  $C^\circ$  is recoverable from the structural triad census as  $C^\circ = 3 \times (t_{30} + t_{31}) / (t_{20} + t_{21} + 3 \times (t_{30} + t_{31}))$ .

*Theorem 2.8 (Existence and uniqueness)*

There exist unique choices of  $X$ ,  $W$ ,  $\mathcal{C}$ , and  $\sim$  that satisfy Axioms 1, 2, and 3. Moreover, these choices also satisfy Axiom 4, and, under them, Eqs. 4 and 5 both produce  $C^\circ$ .

Thm. 2.8 characterizes those specializations of  $\widehat{C}$  that satisfy every axiom.  $C^\circ$  turns out to be the unique such statistic. At the heart of Thm. 2.8 lies the tension between Axiom 2 and Axiom 3. The former forces different types of wedges to be treated differently, and the latter requires that only one of these types figure into the formula.

#### 2.4 Proofs

**Triadic formulations** A different batch of lemmas leads up to each theorem, though note that Thm. 2.7 depends on Thm. 2.6. To simplify the notation, in this section let  $\text{Hom}$  (with no subscript) denote the unspecified  $\text{Hom}_{\mathcal{C}/\sim}$ .

*Proof of Thm. 2.6*

The wedges  $\text{Hom}(W, G)$  can be partitioned according to which triad of  $G$  contains their images. The triads of  $G$  are, in turn, partitioned by the full census. Since the morphisms counts are fixed for isomorphic triads,

$$\widehat{C} = \frac{\sum_{H \subseteq G} |\text{Hom}^X(W, H)|}{\sum_{H \subseteq G} |\text{Hom}(W, H)|} = \frac{\sum_{\mu, w} \left( \sum_{\text{Tr}_{\mu w} \cong H \subseteq G} |\text{Hom}^X(W, \text{Tr}_{\mu w})| \right)}{\sum_{\mu, w} \left( \sum_{\text{Tr}_{\mu w} \cong H \subseteq G} |\text{Hom}(W, \text{Tr}_{\mu w})| \right)} = \frac{\sum_{\mu, w} s_{\mu w} \times S_{\mu w}}{\sum_{\mu, w} s_{\mu w} \times (F_{\mu w} + S_{\mu w})},$$

where  $H \subseteq G$  ranges over the triads of  $G$ .  $\square$

*Lemma 2.9*

Assume Axiom 1.

- i. If  $\text{Tr}_{\mu w}$  has an alcove, then every ordered triple of  $\text{Tr}_{\mu w}$  has an alcove.
- ii. Given actors  $i, j, k \in G$ , there is an openness-preserving bijection between the wedges of  $i, j, k$  and those of  $k, j, i$ .

Part i follows from the symmetry of  $X$ : Whatever the order of the actors, the structure of the triad is the same. Part ii follows analogously from the more limited symmetry of  $W$ , which allows  $v_0, v_1$  to be interchanged with  $v_4, v_3$  with no effect on the structure. (See Fig. 5a,b.)

*Proof*

For i, pick  $\psi \in \text{Hom}(X, \text{Tr}_{\mu w})$  and suppose  $\psi$  takes  $v_0, v_2, v_4$  to  $i, j, k$ . Pick any permutation  $\pi \in S_3$  so that  $\pi(i, j, k)$  is an arbitrary ordered triple in  $\text{Tr}_{\mu w}$ , and let  $\rho_\pi : X \rightarrow X$  be the isomorphism taking  $v_0, v_2, v_4$  to  $\pi(v_0, v_2, v_4)$ , which by Axiom 1 is a morphism. The composition  $\psi \circ \rho_\pi : X \rightarrow \text{Tr}_{\mu w}$  is then a morphism that takes  $v_0, v_2, v_4$  to  $\pi(i, j, k)$ .

For ii, let  $\rho : W \rightarrow W$  be the isomorphism on  $W$  that exchanges  $v_0$  and  $v_4$ , which is a morphism by Axiom 1. Composition with  $\rho$  assigns any wedge  $\phi : W \rightarrow G$  that sends  $v_0, v_2, v_4$  to  $i, j, k$  to a wedge  $\phi \circ \rho$  that sends  $v_0, v_2, v_4$  to  $k, j, i$ . Moreover, since  $\rho \circ \rho$  is the identity morphism on  $W$ , another composition with  $\rho$  takes  $\phi \circ \rho$  back to  $(\phi \circ \rho) \circ \rho = \phi \circ (\rho \circ \rho) = \phi$ . Composition with  $\rho$  thus pairs up the wedges of the triad  $i, j, k$  centered at  $j$  (no wedge is paired with itself). If such a wedge  $\phi$  factors through  $X$  as  $\phi = \psi \circ \iota$ , then  $\phi \circ \rho$  factors through  $X$  as  $\phi \circ \rho = (\psi \circ \iota) \circ \rho = \psi \circ (\iota \circ \rho) = \psi \circ (\rho' \circ \iota) = (\psi \circ \rho') \circ \iota$ , where  $\rho' : X \rightarrow X$  is the isomorphism on  $X$  that exchanges  $v_0$  and  $v_4$ . Thus  $\phi$  and  $\phi \circ \rho$  are open or closed together.  $\square$

The next two lemmas push the binning scheme of Thm. 2.6 from triads to ordered triples. The simplicity of Eq. 7 comes from the fixed number of possible wedges (one for each ordered triple; Axiom 3) and the symmetries between them (Lemma 2.9 and Axiom 4).

*Lemma 2.10*

Assume Axioms 1 and 4. Then, if a triad has two wedges with different centers, then every ordered triple in the triad has an alcove.

*Proof*

By Axiom 4, such a triad has a closed wedge, hence an alcove. By Lemma 2.9i, it then has an alcove at every ordered triple.  $\square$

*Lemma 2.11*

Assume Axioms 1, 3, and 4. Then each triad has exactly one of the following: no wedges, two open wedges, or six alcoves.

*Proof*

Each triad contains six ordered triples, which by Axiom 3 have at most one wedge each. Lemma 2.9ii requires that the wedges centered at any one actor either do not exist, are both open, or are both closed. Lemma 2.10 implies that, if two ordered triples with different centers have wedges, then all six have closed wedges. Thus the possible distributions of wedges among the six ordered triples are none, a pair of open wedges (at the same center), and six closed wedges.  $\square$

*Proof of Thm. 2.7*

Thm. 2.6 provides Eq. 6, which respects triad classes. Lemma 2.11 implies that either  $S_{\mu w} = F_{\mu w} = 0$ ,  $S_{\mu w} = 0$  and  $F_{\mu w} = 1$ , or  $S_{\mu w} = 3$  and  $F_{\mu w} = 0$  for every triad class. Binning these classes into  $S_\emptyset$ ,  $S_W$ , and  $S_X$ , respectively, achieves the result.  $\square$

**Characterization** The characterization theorem takes place over three steps: First, the three assumed axioms only allow wedges and alcoves with no inclusive events ( $\overline{\mathcal{T}}$ ). (This is what makes Axiom 4 unnecessary.) Second, the equal representation of Axiom 3 requires that any wedges at the same ordered triple of actors are congruent ( $\approx$ ), but when inclusive events are ignored the weaker relation  $\simeq$  is enough. This limits the options to the two formulations in Def. 2.4 under the category  $\mathcal{T}/\simeq$ . Third, these formulations agree under certain conditions, which turn out to be satisfied under  $\mathcal{T}/\simeq$ .

*Lemma 2.12*

Assume Axioms 1, 2, and 3. Then any wedge or alcove is an induced injection.

*Proof*

The only way for a wedge or alcove to not be an induced injection is for it to send some event to an inclusive event. Suppose the alcove  $\psi : X \rightarrow G$  sends  $v_0, v_1, v_2, v_3, v_4, v_5$  to  $i, d, j, e, k, f$ , where at least one of the events  $d, e, f$  is inclusive to the triad at  $i, j, k$ . ( $d, e$ , and  $f$  need not be distinct.) If  $d$  or  $e$  is inclusive, then  $\psi \circ \iota : W \rightarrow G$  is a wedge with an inclusive event. If only  $f$  is inclusive, then let  $\rho : X \rightarrow X$  be the isomorphism sending  $v_0, v_1, v_2, v_3, v_4, v_5$  to  $v_2, v_3, v_4, v_5, v_0, v_1$ , so that the composition  $\psi \circ \rho \circ \iota : W \rightarrow G$  sends  $v_0, v_1, v_2, v_3, v_4$  to  $j, e, k, f, i$ . By Axiom 1,  $\psi \circ \rho \circ \iota$  is a wedge with an inclusive event. It is enough, therefore, to prove the result for wedges.



Fig. 6: From the proof of Lemma 2.12: (a) the image of  $\psi : W \rightarrow G$  and (b) the necessary subgraph of  $G$  containing (a).

So suppose the wedge  $\phi : W \rightarrow G$  sends  $v_0, v_1, v_2, v_3, v_4$  to  $i, d, j, e, k$ , where at least one of  $d$  and  $e$  is inclusive to the triad at  $i, j, k$ . Obtain  $G'$  from  $G$  by adding events  $f$ , attended only by  $i$  and  $j$ , and  $g$ , attended only by  $j$  and  $k$ . (See Fig. 6.) The subgraph inclusion  $\sigma : G \rightarrow G'$  is an induced injection, hence by Axiom 1 a morphism. Then the composition  $\sigma \circ \phi : W \rightarrow G'$  is a wedge. The graph map  $\phi' : W \rightarrow G'$  sending  $v_0, v_1, v_2, v_3, v_4$  to  $i, f, j, g, k$  is an induced injection since  $f$  and  $g$  are exclusive events, so by Axiom 1  $\phi'$  is also a wedge—at the same ordered triple as  $\sigma \circ \phi$ . Axiom 2 implies that these wedges are incongruent, which contradicts Axiom 3. Thus  $\phi$  cannot exist.  $\square$

*Lemma 2.13*

Assume Axiom 3. Then  $\sim$  is at least as strong as  $\approx$  on the wedges and alcoves.

*Proof*

The claim is that any two wedges or alcoves on the same ordered triple of actors are congruent. If they were not, then Axiom 3 would be violated.  $\square$

The pullback  $\iota^* : \text{Hom}(X, G) \rightarrow \text{Hom}(W, G)$  sends any alcove  $\psi \in \text{Hom}(X, G)$  to the wedge  $\psi \circ \iota : W \rightarrow G$ . To understand Lemma 2.14, note that the image of  $\iota^*$  is in  $\text{Hom}^X(W, G)$ —that is, each such  $\psi \circ \iota$  factors through  $X$  (via the morphism  $\psi$  began with).

*Lemma 2.14*

Eqs. 4 and 5 yield the same statistic if and only if  $\iota^*$  is injective.

This lemma is not satisfied, for instance, by the category  $\widetilde{\mathcal{T}}/ = \text{underlying } C^*$ : The wedge  $\phi : W \rightarrow \text{Tr}_{(2,1,1),0}$  (Fig. 5d) sending  $v_0, v_2, v_4$  to  $v_2, v_4, v_0$  can be closed by either of the events shared by  $v_0$  and  $v_2$ .  $C^*$ , defined using Eq. 4, counts this as one closed wedge. Its counterpart  $\widehat{C}$ , defined using Eq. 5, however, counts two alcoves, one for each choice of event—that is,  $\phi$  factors through  $X$  in two ways. (Under this statistic, in fact,  $\widehat{C}(\text{Tr}_{(2,1,1),0}) = \frac{6}{5}$ .)

*Proof*

Given  $\phi \in \text{Hom}^X(W, G)$ , by definition there exists  $\psi \in \text{Hom}(X, G)$  such that  $\phi = \psi \circ \iota$ ; thus, in any case,  $\iota^*$  has image  $\text{Hom}^X(W, G)$ . The second condition therefore amounts to  $\iota^*$  being a bijective correspondence between its domain  $\text{Hom}(X, G)$  and its range  $\text{Hom}^X(W, G)$ . Since  $\iota^*$  is surjective and its domain and range are finite, this is true if and only if the domain and range have equal size. Since the denominators of Eqs. 4 and 5 are equal, this is true if and only if the formulations are equal, unless both are undefined. This occurs only when  $\text{Hom}(W, G)$  is empty, in which case both  $\text{Hom}(X, G)$  and  $\text{Hom}^X(W, G)$  are also empty.  $\square$

*Proof of Thm. 2.8*

Lemma 2.12 implies that wedges and alcoves are induced injections. By Axiom 1, all of these are morphisms. As far as Def. 2.4 is concerned, then,  $\mathcal{C}$  is  $\overline{\mathcal{T}}$ .

Lemma 2.13 implies that the congruence relation  $\sim$  is no weaker than  $\approx$ . Since the events of two wedges or alcoves at the same ordered triple must be exclusive, hence structurally equivalent in the triad, the relations  $\simeq$  and  $\approx$  have the same effect in this case;  $\mathcal{C}/\sim$  is  $\overline{\mathcal{T}}/\simeq$ . This establishes uniqueness.

For the auxiliary claim, suppose  $\psi, \psi' \in \text{Hom}_{\overline{\mathcal{T}}/\simeq}(X, G)$  are incongruent. By the choice of  $\overline{\mathcal{T}}$ , their respective images of  $v_1, v_3, v_5$  must be exclusive. If  $\psi, \psi'$  agree on all three actors, then, by the choice of  $\simeq$ , they are congruent. So  $\psi, \psi'$  must disagree on some actor; say  $\psi(v_0) \neq \psi'(v_0)$ . This implies that  $\psi \circ \iota(v_0) = \psi(v_0) \neq \psi'(v_0) = \psi' \circ \iota(v_0)$ , hence that  $\iota^*(\psi) \neq \iota^*(\psi')$ . Thus,  $\iota^*$  is injective. By Lemma 2.14, both formulations of Def. 2.4 produce the same statistic.

It remains to verify that  $C^\circ$  actually satisfies each axiom; this is left to the reader.  $\square$

### 3 Empirical analyses

This section brings the statistics  $C$ ,  $C^*$ , and  $C^\circ$  together with three empirical networks to perform two, in some sense dual, analyses: First, Sec. 3.1 assesses the clustering coefficients as measurement instruments, using the empirical networks as a stage on which to compare their performances. The assessments draw upon both local and global samples and are illustrated through two specific cases. Second, Sec. 3.2 takes the empirical networks as its objects of study. Several analyses use the census and the clustering coefficients to explore the varieties of TC and their relationships to the strength of personal connections, the connectivity of neighborhoods, and the centrality of actors. In the process, concepts from previous studies (see Sec. 1.1) are extended to the AN setting.

#### 3.1 Instrumentation

**Data** The analyses employ three empirical networks: The social activity attendance network DDGGS1 comes from another table in the same study as above (Davis *et al.*, 1941), and has seen extensive use as an illustration for node classification and community detection techniques (Freeman, 2003). A subset of interlocking directorates data, from a study of corporate philanthropy in Minneapolis–St. Paul (Galaskiewicz, 1985; Wasserman & Faust, 1994), constitute GWF, which has also seen wide use as an example (Scholtens, n.d.). Finally, MR refers to the collaboration network constructed from the *Mathematical Reviews* bibliographic database, which is maintained by the American Mathematical Society, over the years 1985–2008. These networks were chosen for three reasons: they are constructed from a range of types and volumes of social interaction data; the networks have appeared in previous studies that provide checks and comparisons for the present work; and two (DDGGS1 and MR) are dynamic.<sup>12</sup>

<sup>12</sup> DDGGS1 is assumed here to consist of events spanning nine months (Freeman, 2003); however, whereas the study took place over two years (Davis *et al.*, 1941), other orderings of the dates are possible, and no confirmatory source is known to the author.

Table 2: Structural censuses of DDGGS2, DDGGS1, GWF, and two intervals of MR. The columns indicate the presence (1) or absence (0) of an inclusive event; the row indicates the number of pairs of actors who attend at least one exclusive event.

		DDGGS2		DDGGS1		GWF		MR (1985-7)		MR (2005-7)	
		0	1	0	1	0	1	0	1	0	1
0	0	0	0	17	0	284	80747526018836	17275	725892036097769	76558	
1	0	1	39	240	266	886	4721138210	8611	38496757064	51599	
2	3	3	146	253	452	521	133630	2014	909505	15185	
3	3	0	45	76	130	61	886	129	5585	1055	

Table 2 presents the structural censuses of the networks. The structure revealed in the second column of each census is structure gained by taking the direct approach, rather than projecting to a traditional network. Several differences between DDGGS1 and GWF, on one hand, and MR, on the other, are apparent: MR is far larger, with triads concentrated among the less-connected; “symmetric exclusive” triads ( $t_{30}$ , see Ex. 2.3) make up a minuscule fraction. In contrast, DDGGS1 and GWF have remarkably similar profiles, also similar to that of DDGGS2: the event-free triads number  $t_{00} = 0$ , and the largest tallies occupy a northeast–southwest diagonal band away from the least and most connected types. This indicates that the smaller networks are more uniformly connected, with fewer “leaf” (having only one neighbor) and isolated actors. This difference likely reflects non-uniformity in the coverage of researchers in MR (Lee & Cunningham, 2013), e.g. as researchers on the periphery of mathematics appear less frequently in MR.

For the purpose of the assessments, a family of dynamic networks is drawn from MR. The editors assign to each publication one primary and any number of secondary Mathematical Subject Classification (MSC) codes from a hierarchical scheme. At the coarsest level, publications are binned into 64 groups (for instance, algebraic geometry and partial differential equations). Sixty-four subnetworks can then be constructed by partitioning the literature according to primary classification. Of these subnetworks, 39 satisfy the following inclusion criteria over each adjacent 3-year interval from 1985–7 to 2006–8: the literature is not empty; each of  $C$ ,  $C^*$ ,  $C^\circ$ , and  $D$  is defined; and no two of these statistics are zero. Since their curation and construction are systematic, differences in structure among these networks should only reflect differences in the cultures of research publication and their overlap with MR coverage. (Note, though, that size and density are known to influence global statistics.)

**Criteria** While the statistics surveyed in Sec. 1.2 make intuitive sense, an important step separates the design of a measurement instrument from its application to empirical questions, namely the assessment of its practical use as an instrument.<sup>13</sup> This section assesses  $C$ ,

<sup>13</sup> Strictly speaking, the “instrument” that assigns a clustering coefficient to a social network includes the collection of sociometric data and the construction of the bipartite graph as well as the graph-

$C^*$ , and  $C^\circ$  on the basis of four criteria—stability, concurrent validity, discriminability, and distinguishability—in terms of variance. The assessments are performed on three samples: the 18 actors of DDGGS1, the 26 actors of GWF, and the 39 disciplines of MR (on each of the eight adjacent 3-year intervals). The criteria are conceptualized and assessed as follows:

- An instrument is *stable* (or test–retest reliable) if it yields similar measurements of the same subject at different times. Stability is assessed, on pairs of values at the same MR discipline at adjacent intervals, as the proportion  $\frac{SSM}{SST}$  of the variation in the values accounted for by the pairing in a one-way analysis of variance (Altman & Bland, 1983). (Adjacent intervals minimize the effect of network evolution.)
- Both  $C^*$  and  $C^\circ$  are hypothesized to measure properties of graphs that can also be measured in other ways: As mentioned in Sec. 1.2, an alternative correction to  $C$  for event size in ANs is the quotient of  $C$  by its expected value  $C_{\text{rand}}$  on an equivalent random bipartite graph.<sup>14</sup> Sec. 1.2 also suggested that  $C^\circ$  indirectly measures dynamic TC, defined as  $D$ . The *concurrent validity* of each measure shall be assessed as its coefficient of determination  $R^2$  with the corresponding alternative—that is, the proportion of total variance in one measure explained (via linear regression) by the other (Kimberlin & Winterstein, 2008).
- Two instruments designed to measure distinct properties shall be called *distinguishable* if they yield divergent values on the same subjects. Whereas the coefficient of determination between these values could be interpreted (as above) as their concurrent validity, the remaining proportion of variance,  $1 - R^2$ , shall be used to assess their distinguishability from each other.
- Discriminability is not a measure of reliability or validity but of usefulness. An instrument is *discriminable* if the values it takes in practice are dispersed throughout its theoretical range (Comin *et al.*, 2014). (Sec. 1 criticized  $C$  for having low discriminability on ANs.) Discriminability is assessed as the variance  $\sigma^2$  of an instrument’s values for a sample of subjects; whereas the maximum possible variance on  $[0, 1]$  is  $\frac{1}{4}$ , the standardized values  $\sigma^2/\frac{1}{4} = 4\sigma^2$  are reported. Thus discriminability ranges, in theory, from 0 (all values equal; statistic is of no use) to 1 (values evenly split between 0 and 1; statistic perfectly dichotomizes the subjects); a statistic whose values are evenly spread throughout  $[0, 1]$  has discriminability  $\frac{2}{3}$ .

On MR, each assessment is performed on the pooled values across all intervals. For instance, each statistic’s stability is computed on  $39 \times 7 = 273$  ordered pairs of values, one for each discipline and each adjacent pair of years.

**Results** The test results constitute Table 3. (Empty cells correspond either to nothing meaningful or to duplicate values. Plots for each assessment on MR are included in the supplement.)  $C$  is by far the most stable of the statistics ( $\frac{SSM}{SST} = 0.78$ ), with less than half

theoretic calculation and the device that performs it; the present discussion is restricted to the design of the calculation.

<sup>14</sup> Here  $C_{\text{rand}}$  is calculated two ways: For the smaller networks DDGGS1 and GWF, take the mean (local) values of  $C$  across 1000 randomly generated bipartite graphs having the same actor and event degree sequences (Chen *et al.*, 2005; Admiraal & Handcock, 2008). For the larger MR subnetworks, use the asymptotic approximation (Newman *et al.*, 2001).

Table 3: Evaluations of three clustering coefficients taken over actors (DDGGS1 and GWF) or subnetworks (adjacent 3-year intervals of MR).

	Classical			Opsahl			Exclusive		
	DDGGS1	GWF	MR	DDGGS1	GWF	MR	DDGGS1	GWF	MR
Stability			0.781			0.403			0.457
Validity				0.619	0.291	0.113	0.058		0.399
Dist. (Classical)				0.950	0.940	0.999	0.492	0.732	0.924
Dist. (Opsahl)							0.915	0.592	0.948
Discriminability	0.005	0.013	0.047	0.051	0.050	0.026	0.205	0.224	0.001

of the variation in  $C^*$  and  $C^\circ$  each interval explained by the previous. Tests of validity were inconsistent.  $C^*$  was highly correlated with  $C/C_{\text{rand}}$  across the women of DDGGS1, but less so across the CEOs of GWF and not at all across the disciplines of MR. Conversely,  $C^\circ$  explained half of the variance in  $D$  across the disciplines but essentially none across the women. There is strong evidence here that these pairs of instruments are closely related in certain settings, but also that they are not concurrently valid in general.<sup>15</sup> Plots reveal increasing variation in  $C^\circ$  with increasing value, which is further cause for caution.

The three statistics are highly distinguishable with respect to each other; at worst,  $C$  explains half of the variance in  $C^\circ$  on the actors of DDGGS1 ( $1 - R^2 = 0.49$ ). This, residual plots reveal, is due to a slight but consistent negative relationship. None, however, are consistently discriminable; moreover, discriminability seems to depend heavily on the network type:  $C^\circ$  is most discriminating of the actors ( $4\sigma^2 = 0.2$ ), followed by  $C^*$  and  $C$ ; and the order is reversed for the subnetworks of MR, with  $C$  most discriminating among them ( $4\sigma^2 = 0.05$ ). This makes sense in light of the higher average rates of TC in DDGGS1 and GWF; while MR includes many highly connected triads, they are overwhelmed by the more partially connected, which  $C$  is better-equipped to parse. Overall, the assessments lend some credibility to the uses of  $C$ ,  $C^*$ , and  $C^\circ$  in the next section, but there remains a need for more persuasive assessments of single-value network statistics.

### Example 3.1

Consider the TC of the women who constitute DDGGS1 (Table 4, with structural equivalents Olivia and Flora represented by Olivia; centrality scores are used later in Sec. 3.2. The supplement contains an analogous table for GWF). Partitioning and core–periphery algorithms tend to identify Pearl, Ruth, and Verne as intergroup bridges or peripheral group members (Freeman, 2003), though in terms of classical TC their neighborhoods are typical. In contrast, these women exhibit the lowest Opsahl TC of the group, and two (Ruth and Verne) are among the three with lowest exclusive TC. These observations are made possible by the greater discriminability of these statistics.

<sup>15</sup> These inconsistencies suggest that the proliferation of 3-edge triads in ANs has more sources than the two identified here (large bicliques and dynamic triadic closure). This would be an interesting counterpoint to the observation that the higher-than-expected triangle frequency in traditional empirical networks is driven by mid-size cliques (Slater *et al.*, 2014).

Table 4: Measures of local triadic closure and centrality in DDGGS1.

	Classical	Opsahl	Exclusive	Dynamic	TwoPath	Eigenvector	FourPathCorrected
Evelyn	0.897	0.767	0.448	0.576	0.319	0.335	0.011
Laura	0.962	0.842	0.487	0.692	0.286	0.309	0.015
Theresa	0.897	0.752	0.145	0.650	0.358	0.371	0.009
Brenda	0.962	0.839	0.450	0.692	0.292	0.313	0.015
Charlotte	1.000	1.000	1.000	1.000	0.154	0.168	0.010
Frances	0.962	0.869	0.778	0.000	0.198	0.209	0.008
Eleanor	0.962	0.796	0.531	0.692	0.220	0.228	0.006
Pearl	0.933	0.646	0.467	0.636	0.187	0.180	-0.004
Ruth	0.897	0.670	0.328	0.650	0.242	0.236	-0.003
Verne	0.897	0.674	0.393	0.576	0.231	0.218	-0.009
Myra	0.933	0.714	0.556	0.273	0.204	0.187	-0.012
Katherine	0.933	0.770	0.536	0.273	0.237	0.220	-0.013
Sylvia	0.897	0.746	0.300	0.576	0.292	0.277	-0.012
Nora	0.897	0.838	0.663	0.725	0.281	0.264	-0.013
Helen	0.897	0.816	0.661	0.611	0.215	0.201	-0.010
Dorothy	0.933	0.541	0.467	0.000	0.143	0.131	-0.007
Olivia	1.000	0.581	1.000	1.000	0.088	0.070	-0.011

Pearl, however, has exclusive TC on par with several women in the cores of the two communities (Evelyn, Laura, and Dorothy). Theresa and Sylvia, on the other hand—who are usually placed near the cores of their respective groups within DDGGS1, rather than toward the periphery with Ruth and Verne—show lower exclusive TC. This is due to the high number of events (8 and 7) these women attended; it may be that measurements were cut too short in time for their neighbors to have attended more events in their absence, though this is unlikely, since both women attended events as early as March and as late as September; or it may be that these women played distinctive networking roles in their respective groups, to which traditional algorithms are not sensitive (see Sec. 3.2).

### Example 3.2

A previous study of MR (Brunson *et al.*, 2014) compared two subnetworks, constructed from a nearly even partition of the literature by MSC into “pure” and “applied”, against the aggregate network and each other over time.<sup>16</sup> The analysis of TC used  $C$  and  $C/C_{\text{rand}}$ ; the time series are reproduced in Fig. 7 (“Classical” and “BipartiteCorrected”). While  $C$  revealed persistent properties of MR, e.g. that the applied research community saw more classical TC than the pure,  $C/C_{\text{rand}}$  measured TC that had been on the rise in pure research but not in applied. Both statistics arguably discriminated well, and certainly they were distinguishable from each other:  $C/C_{\text{rand}}$  was responsive to significant changes in the networks relative to each other, while  $C$  measured something more permanent.

<sup>16</sup> The partition is coarse and provisional, but reflects a real difference between the research cultures; these subnetworks displayed consistently and characteristically different behavior.

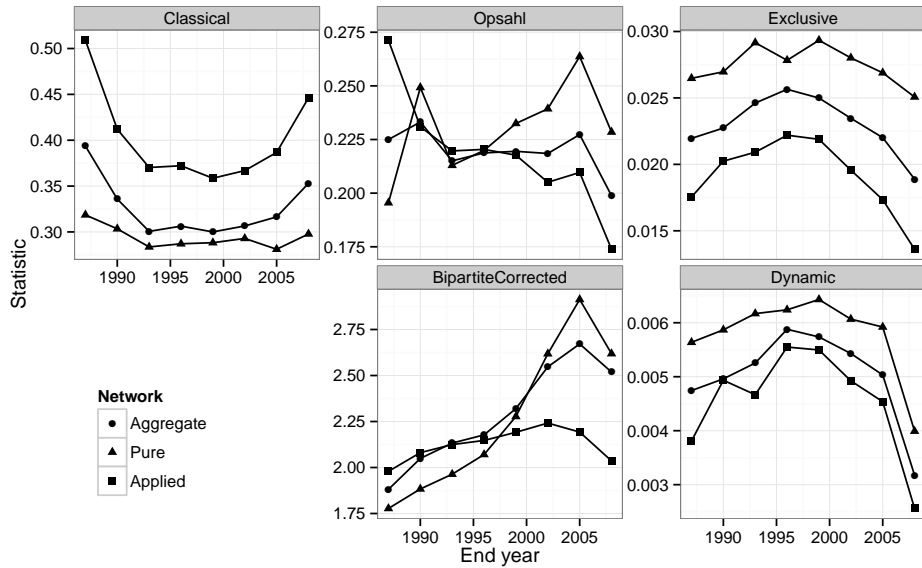


Fig. 7: Three global clustering coefficients and alternative measures for two, on the aggregate, pure, and applied MR networks along adjacent 3-year intervals.

Fig. 7 also includes time series for  $C^*$  and  $C^\circ$ :  $C^*$  mimics  $C/C_{\text{rand}}$  moderately closely; both show rising TC in pure research and progressively lower rates in the aggregate and in the applied. They differ in that  $C/C_{\text{rand}}$  detects a rising influence that  $C^*$  does not. More impressive is the predictive power of  $C^\circ$  on  $D$ ; their time series are very similar.  $C^*$  and  $C^\circ$  both are less discriminating than  $C$  in absolute terms, though all three are clearly distinguishable. Like  $C$ ,  $C^\circ$  measures a persistent difference between the research cultures: Pure research is better characterized by exclusive TC than applied. The negative relationship between  $C$  and  $C^\circ$  is evident here, as the relative values of  $C^\circ$  are inverted from those of  $C$ , both in the ordering of the networks and in the concavity of the time series.

### 3.2 Triadic closure in affiliation networks

**Strong triadic closure** In social networks with ties of different strengths, the STC hypothesis (Sec. 1.1) predicts that, when two pairs of actors in a triad are *strongly* tied, then the third pair will, with greater probability, be at least *weakly* tied (Granovetter, 1973). Investigators have formalized and tested this principle in a variety of ways, often in terms of the frequency, duration, or intimacy of relations, or of the proportion of relations that surpass some threshold of strength (Freeman, 1992). One conversion approach to STC in ANs is therefore to apply these methods to a weighted projection.

The full triad census offers a direct approach: It makes sense to infer stronger ties between actors in a triad from exclusive events between them than from inclusive events, consistent with the principle that higher-attendance events foster weaker pairwise connections (Gupte & Eliassi-Rad, 2012). Accordingly, take the *wedge strength* of the ordered triple  $(i, j, k)$  to be the number of 4-paths along exclusive events from  $i$  through  $j$  to  $k$ , and

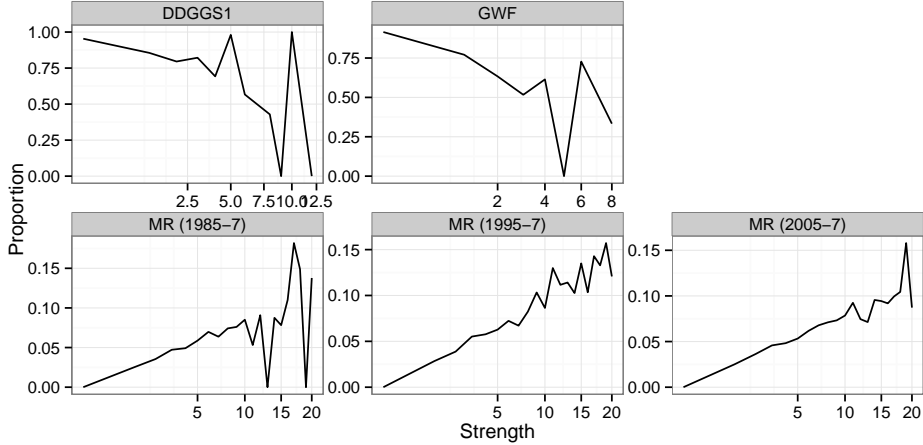


Fig. 8: Conditional probability  $\Pr(\mu_3 + w > 0 | \mu_1 \times \mu_2 = s)$  of a weak tie versus tie strength  $s$ , up to  $s = 20$ . (Note the square root-scale horizontal axis.)

take  $i$  and  $k$  to be (*at least*) *weakly tied* if there is some 2-path between them. Thus, the triple  $p, q, r$  in the triad  $\text{Tr}_{\mu w}$  have wedge strength  $\mu_1 \times \mu_2$  and are weakly tied if  $\mu_3 + w > 0$ . One may then compute the STC of an affiliation network as the conditional probability of a weak tie on wedge strength.<sup>17</sup>

Fig. 8 presents the conditional probabilities for DDGGS1, GWF, and MR over three evenly-spaced 3-year intervals, using a square-root scale on the horizontal axis. The negative relationship in DDGGS1 and GWF belies STC; increasing wedge strength is associated with a lower rate of weak tie formation, though the relationship is noisy. In contrast, STC in MR is well-modeled by the proportionality relationship

$$\Pr(\mu_3 + w > 0 | \mu_1 \times \mu_2 = s) \propto s^{\frac{1}{2}}. \quad (8)$$

Furthermore, though STC makes no predictions about the proportion of ties between actors who do not have a specific neighbor in common (the case  $s = 0$ ), in MR this singular case is well-extrapolated from the pattern across wedges of positive strength. Also noteworthy in MR is that the constant  $s$  appears stable over time, with transient rather than persistent fluctuations. This indicates that Eq. 8 is robust.

**Connectedness and constraint through coattendance** The STC hypothesis is intimately tied to the concept of structural holes (Burt, 1992): The better-connected an actor's neighborhood, the less strategic their position; connections among neighbors constrain the actor's capacity to broker exchanges between them. The classical clustering coefficient provides a coarse approximation to this concept: The constraint of actor  $j$  on actor  $i$  is the product of (a)  $i$ 's investment in reaching  $j$  and (b)  $j$ 's connectedness (within  $i$ 's neighbor-

<sup>17</sup> An alternative measure of STC is the expected mean number of events attended by  $i$  and  $k$ , conditioned on the wedge strength of  $(i, j, k)$ . The results in MR, not reported, closely match those shown for the conditional probability.

hood). In the traditional network setting, if  $i$  has  $d$  neighbors (including  $j$ ), then about  $\frac{1}{d}$  of  $i$ 's investment is in  $j$ . Meanwhile,  $j$  may be tied to anywhere from 0 to  $d - 1$  of  $i$ 's other neighbors; call this number  $d(j)$ . The constraint on  $i$  due to  $j$  is then

$$c(i, j) = \frac{1}{d} \times \frac{d(j)}{d-1} = \frac{d(j)}{d(d-1)},$$

and the total constraint on  $i$  is  $c(i) = \sum_j c(i, j) = \sum_j d(j)/d(d-1) = (\sum_j d(j)/2)/\binom{d}{2}$ , which is the local clustering coefficient  $C(i)$ . An alternative formulation interprets  $i$ 's investment and  $j$ 's isolation in terms of wedges centered at  $i$  and involving  $j$ :

$$c(i, j) = \frac{|\{\text{wedges at } i \text{ w/ } j\}|}{|\{\text{wedges at } i\}|} \times \frac{|\{\text{closed wedges at } i \text{ w/ } j\}|}{|\{\text{wedges at } i \text{ w/ } j\}|} = \frac{|\{\text{closed wedges at } i \text{ w/ } j\}|}{|\{\text{wedges at } i\}|}. \quad (9)$$

Eq. 9 generalizes neatly to the terms of Def. 2.4, Eq. 4, so that this coarse conception of constraint specializes to a range of statistics for ANs.

This presents an opportunity to explore the highly-studied relationship between constraint and neighborhood size. As usually defined, constraint decreases with neighborhood size (Burt, 1992). This is resonant with the power law relationship

$$C_\ell \propto \ell^\gamma \quad (10)$$

between the number  $\ell$  of wedges centered at an actor and the wedge-dependent local clustering coefficient, which has been well-documented in both theoretical (Dorogovtsev *et al.*, 2002; Szabó *et al.*, 2003) and empirical (Ravasz *et al.*, 2002; Vázquez, 2003) settings.<sup>18</sup> In contrast, if the proportional investment of  $i$  in  $j$  is replaced with  $i$ 's marginal investment in  $j$  (that is,  $i$ 's investment in  $j$  as a fraction of the maximum investment of  $i$  in any neighbor), then constraint increases with neighborhood size *and density*, under a powerful interaction effect (Burt, 1992). The two versions of constraint reflect two understandings of  $i$ 's strategic position: as relying on *exclusive* connections with neighbors versus on *shared* connections.

This distinction translates naturally into AN triad terms: First, rather than the number of neighbors, use the number of wedges centered at  $i$  as a proxy for neighborhood size.<sup>19</sup> Then, for any choices of  $X$ ,  $W$ ,  $\mathcal{C}$ , and  $\sim$  in Def. 2.4, the relationship between constraint and neighborhood size is borne out as the wedge-dependent clustering coefficient  $\widehat{C}_\ell$ .  $\widehat{C}_\ell$  should decrease (or increase less) with  $\ell$  when inclusive events play a smaller role—for instance, when  $X$  and  $W$  have more exclusive events, i.e.  $X = \text{Tr}_{(1,1,0),1}$  or  $X = \text{Tr}_{(1,1,1),0}$ , and when graph maps are induced, i.e.  $\mathcal{C} \subseteq \mathcal{T}$ . In networks with high rates of repeat coattendance, the role of inclusive events can also be reduced by imposing a strong congruence relation, e.g.  $\simeq$  or  $\approx$ .

Of the statistics under consideration, then,  $C^*$  is best-poised to measure constraint based on marginal investment. A natural counterpart  $C^+$ , to measure constraint based on proportional investment, can be adapted from  $C^*$  by restricting the graph maps to induced injections—that is, by eliminating any role for inclusive events. Fig. 9 depicts  $C_\ell^*$  and  $C_\ell^+$

<sup>18</sup> Eq. 10 is usually presented as  $C_k \propto k^\gamma$ , where  $k$  is actor degree. Asymptotically, taking  $\ell = k(k-1)$ , this translates to  $C_\ell \propto \ell^{\frac{\gamma}{2}}$ .

<sup>19</sup> This could be likened to measuring the “effective size” of  $i$ 's neighborhood (Burt, 1992).

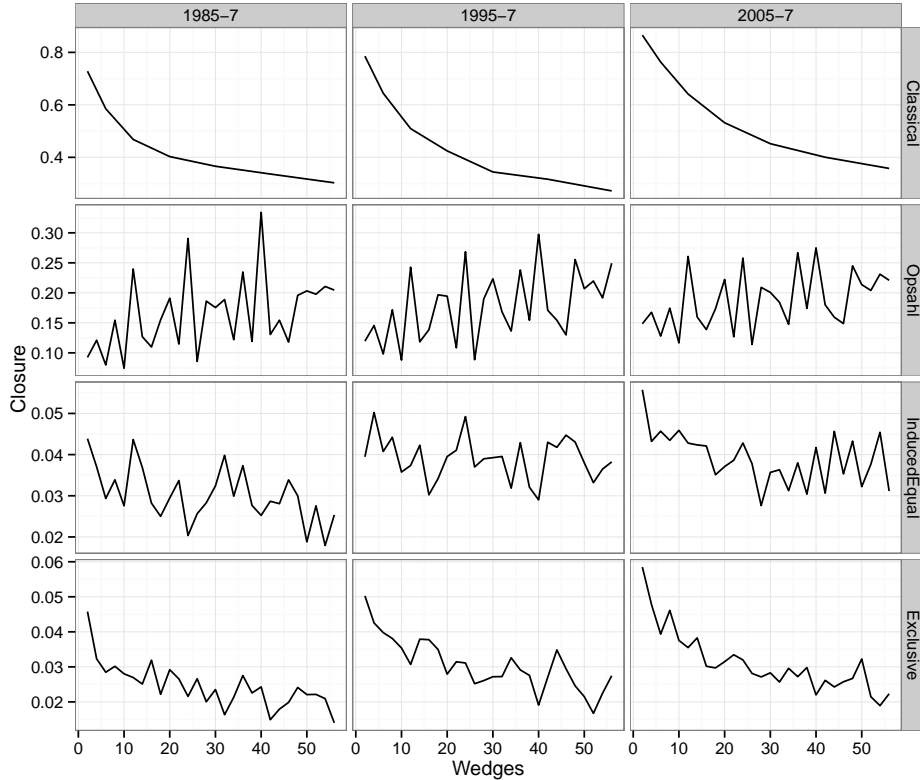


Fig. 9: Four wedge-dependent local clustering coefficients in MR. Note that  $C_\ell$  is only defined when  $\ell = k(k-1)$  for some integer  $k$ .

on MR, taken over the same three intervals as in Sec. 3.2.<sup>20</sup> Since  $C^\circ$  is closely related to  $C^+$  (it obtains from imposing the congruence relation  $\simeq$ ), and since the classical  $C_\ell$  provides an important backdrop, both are included for comparison.  $C_\ell$  follows the expected power law-shaped curve, which persists over time. In contrast, the long-term trend in  $C_\ell^*$  is upward, and exhibits large fluctuations with persistent peaks (e.g. at  $\ell = 12$  and  $\ell = 24$ ).  $C^+$  fluctuates at a lower rate (notice the vertical scales) and with more transient peaks, following a perceptibly downward trend.  $C_\ell^\circ$  most closely mimics  $C_\ell$ : The long-term trend is downward and concave, and the fluctuations are modest and transient.

The persistent peaks in  $C_\ell^*$  are an expected artifact of a high occurrence of bicliques (see Sec. 1.2): Whenever  $n \geq 3$  and  $m \geq 2$ , the biclique  $K_{n,m}$  yields, for each of its actors  $j$ , pairs of neighbors and  $m(m-1)$  ordered pairs of events they share with  $j$ , resulting in  $(n-1)(n-2) \times m(m-1)$  4-paths centered at  $j$ . When  $m \geq 3$ , each of these is closed by a third event. Thus, any otherwise untied actor in a copy of  $K_{n,m}$  contributes the atypically high value  $C^*(j) = 1$  to the mean  $C_\ell^*$ , where  $\ell = (n-1)(n-2) \times m(m-1)$ . These values  $\ell = (3-1)(3-2) \times 3(3-1) = 12$ ,  $\ell = (3-1)(3-2) \times 4(4-1) = 24$ ,  $\ell = (4-1)(4-$

<sup>20</sup> Scatterplots of  $\hat{C}_\ell$  versus  $\ell$  in DDGGS1 and GWF are included in the supplement.

$2) \times 3(3-1) = 36$ , and  $\ell = (3-1)(3-2) \times 5(5-1) = 40$  correspond to the highest peaks of  $C_\ell^*$  up to  $\ell = 56$ .<sup>21</sup>

The results are mostly consistent with expectations:  $C^*$  may be an appropriate (though still coarse) measure of marginality constraint, and  $C^+$  or  $C^\circ$  one of proportionality constraint; though wedge-dependent values  $C_\ell^*$  must be compared with caution, due to the influence of bicliques. The structure of MR exhibits two clear trade-offs: First, as observed in other settings, the proportional connectedness (in terms of  $C$ ) among a researcher's collaborators diminishes with their number. Second,  $C_\ell^\circ$  shows that the level of *exclusive* connectedness among a researcher's collaborators diminishes with the number of *irredundant* pairings among them. Since exclusivity is important to the theory of structural holes, this may point to a more proper test of that theory for ANs.

**Exclusivity and influence** The discussion of brokerage can be taken a step further, to examine actors' outreach and influence beyond their immediate neighborhoods, while keeping one foot planted in the realm of triads: The numerator of Eq. 4 may be interpreted as the number of redundant 6-paths emanating from an actor  $i$ , i.e. those that form 6-cycles. If, as above, the denominator is interpreted as a measure of  $i$ 's outreach effort, then  $\hat{C}$  may be viewed as a constraint on  $i$ 's extended influence through 6-paths (and the longer paths that rely on them). One should expect, therefore, to find a negative relationship between  $i$ 's influence *due to paths of length (at least) 6* and the number of closed wedges centered at  $i$ —for a suitable definition of wedge. The following analysis considers  $C^*$  and  $C^\circ$ .

What is needed is a measure of extended influence. Influence is often measured using eigenvector centrality, which is based on the recursive principle that an actor accumulates influence through connections with other influential actors. This measure has been directly applied to ANs (Faust, 1997; Borgatti & Halgin, 2011). Additionally, eigenvector centrality was the basis for a proposed measure of influence through paths of at least a specified length (Bonacich, 1991): Given an AN  $G$  with  $n$  actors and  $m$  events, let  $A$  be its  $n \times m$  incidence matrix, so that  $B = AA^\top$  is the (weighted)  $n \times n$  coattendance matrix for the actors. The  $i^{\text{th}}$  row (or column) sum  $b_1(i)$  of  $B$  is then the “2-path centrality” score of  $i$ , which equals  $i$ 's weighted degree centrality in the projection. The eigenvector centrality score of  $i$  is obtained by first computing the matrix  $E = \lim_{\beta \rightarrow \frac{1}{\lambda}} \sum_{t=1}^{\infty} \beta^{t-1} B^t$ , where  $\lambda$  is the largest eigenvalue of  $B$ , then taking the  $i^{\text{th}}$  row sum of  $E$ . Interpolating between these extremes are the  $2\ell$ -path centrality scores  $b_\ell(i)$ , given by the  $i^{\text{th}}$  row sum of  $\sum_{t=1}^{\ell} \beta^{t-1} B^t$ , which incrementally incorporate  $i$ 's influence due to longer and longer paths.

To draw meaningful comparisons between these scores, they are standardized as follows: Let  $\mathbf{b}_\ell$  denote the vector of  $2\ell$ -path centrality scores across all actors of  $G$ . Let  $\mathbf{c}_\ell = \mathbf{b}_\ell / \sum_{i=1}^n b_\ell(i)$ , the unit vector, in  $n$ -dimensional space, pointing in the same direction as  $\mathbf{b}_\ell$ . Since  $c_\ell(i)$  measures  $i$ 's influence due to paths of length at most  $2\ell$ , and the analogously defined  $c_\infty(i)$  (standardized eigenvector centrality) measures  $i$ 's influence due to all paths,  $i$ 's influence due to paths of length *at least*  $2\ell$  can be measured as  $c_\infty(i) - c_{\ell-1}(i)$  (which

<sup>21</sup> Two other clustering coefficients derived from Eq. 2.4, based on  $\widetilde{\mathcal{T}}/\simeq$  and  $\widetilde{\mathcal{T}}/\approx$ , were tested for wedge-dependent closure (not reported). Both exhibited persistent fluctuations, which were also expected from clique proliferation, but downward long-term trends.

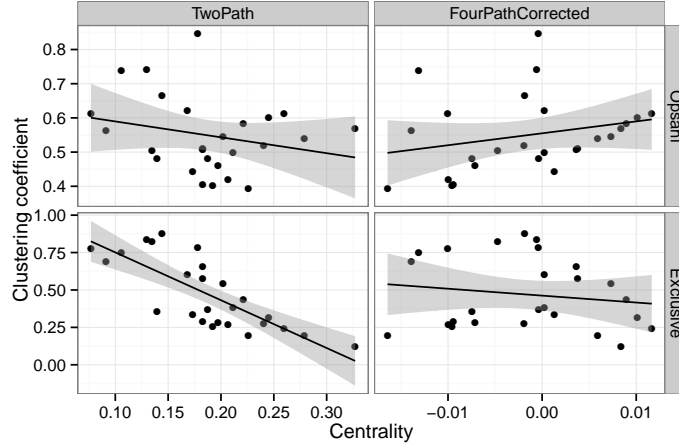


Fig. 10: Scatterplots of Opsahl and exclusive clustering coefficients versus 2-path and 4-path-corrected eigenvector centrality scores across actors in GWF. Least-squares regression lines and 95% confidence bands are overlaid.

will take positive and negative values). The centrality score of interest at present is then  $c_\infty - c_2$ , or *4-path-corrected eigenvector centrality*, and the hypothesis posed is that  $C^*$  or  $C^\circ$  should be anti-correlated with  $c_\infty - c_2$ .

Fig. 10 plots the local clustering coefficients  $C$ ,  $C^*$ , and  $C^\circ$  against  $c_1$  and  $c_\infty - c_2$  for the CEOs of GWF. (The corresponding plots for the women of DDGGS1, included in the supplement, are very similar.) The data clearly refute the hypothesis. There is essentially no relationship, across either set of actors, between extended influence and TC. There is instead a strong relationship in both networks between influence and exclusive TC (not shown); but this is due entirely to influence due to 2-paths. The linear model

$$C^\circ(i) = \beta_0 + \beta_1 c_1(i) + \varepsilon_i, \quad (11)$$

with Gaussian errors  $\varepsilon_i$ , fits the data reasonably well. An increase in 2-path centrality of 0.1 corresponds to a decrease of 0.46 (GWF) or 0.31 (DDGGS1) in  $C^\circ$ . This is not unexpected in light of the constraint discussion. However, when this analysis pairs an explicitly non-local measure of influence with a purely local measure of connectivity and cohesion, no relationship is detected.

#### 4 Conclusion

This paper was motivated by the need for a measure of triadic closure for affiliation networks that controls for the influence of repeat event attendance by actors, which manifests as biclique proliferation. The proposed exclusive clustering coefficient  $C^\circ$  also assigns equal weight to all actors, as the classical clustering coefficient,  $C$ , does. The paper presented a classification scheme for triads and a generic clustering coefficient, which aided in assessing the theoretical qualities of the huge range of possible statistics, including several already proposed. This was done through an axiomatic approach. In addition to

$C^\circ$ , this process yielded the structural triad census, a compact summary that reveals useful affiliation structure absent from the simple census. An instrumental analysis found  $C^\circ$  and the recent proposal  $C^*$  to be distinct from  $C$ , and provided evidence that  $C^\circ$  approximates dynamic triadic closure in some settings. An investigation into triadic closure in empirical affiliation networks, using  $C$ ,  $C^*$ , and  $C^\circ$ , revealed patterns of structure and behavior that  $C$  alone could not. Overall, the results depict  $C^\circ$  in particular as a counterpoint to  $C$ ; the two could be viewed as limiting cases, from most to least restrictive of what arrangements of events contribute to triadwise connectivity, between which other clustering coefficients like  $C^*$  interpolate (Saramäki *et al.*, 2007).

The present study has several limitations and suggests several other avenues for future work: The range of possible specializations of Def. 2.4 may encourage studies of specifically-tailored notions of triadic closure; though many of the tools introduced here are computationally expensive and require more efficient implementations or approximations. The structural triad census could, like the simple census, provide the basis for a state transition analysis to affiliation network triads (Doroud *et al.*, 2011; Juszczyszyn *et al.*, 2011), and would also benefit from comparison to a suitable null model (Davis, 1970; Faust, 2008). It is also important to note that the empirical analyses of Sec. 3 used only three networks, so that there is much room to challenge the conclusions drawn here. In summary, it is hoped that the present paper provides a useful, unified framework for an ongoing triadic analysis of affiliation networks.

**Acknowledgments** The author thanks Ritchie C. Vaughan for suggesting this line of inquiry; to Miranda Lynch, Tina Eliassi-Rad, Roldan Pozo, Paola Vera-Licona, Linton Freeman, Kathy O’Hara, and Reinhard Laubenbacher for helpful conversations; to Barry Brunson and Pansy Waycaster for several rounds of proofreading; to three anonymous reviewers for highly incisive and supportive comments; and to the Virginia Bioinformatics Institute, the AMS, and UConn Health for data and resources. This project builds upon work done by participants in the Summer 2010 REU in Modeling and Simulation in Systems Biology.

## References

Admiraal, Ryan, & Handcock, Mark S. (2008). networksis: A package to simulate bipartite graphs with fixed marginals through sequential importance sampling. *Journal of statistical software*, **24**(8), 1–21.

Altman, Douglas G., & Bland, J. Martin. (1983). Measurement in Medicine: The Analysis of Method Comparison Studies. *The statistician*, **32**(3), 307–317.

Bonacich, Phillip. (1991). Simultaneous group and individual centralities. *Social networks*, **13**, 155–168.

Bondy, J. Adrian, & Murty, U.S.R. (2008). *Graph theory*. Graduate texts in mathematics. Springer.

Borgatti, Stephen P., & Halgin, Daniel S. (2011). Analyzing affiliation networks. Pages 417–433 of: Scott, John, & Carrington, Peter J. (eds), *The sage handbook of social network analysis*. SAGE Publications Ltd.

Breiger, Ronald L. (1974). The Duality of Persons and Groups. *Social forces*, **53**(2), 181–190.

Brunson, Jason Cory, Fassino, Steve, McInnes, Antonio, Narayan, Monisha, Richardson, Brianna, Franck, Christopher, Ion, Patrick, & Laubenbacher, Reinhard C. (2014). Evolutionary events in a mathematical sciences research collaboration network. *Scientometrics*, **99**(3), 973–998.

Burt, Ronald S. (1992). *Structural holes: The social structure of competition*. Cambridge, MA: Harvard University Press.

Carrino, Christopher N. (2006). *A study of repeat collaboration in social affiliation networks*. Ph.D. thesis, University Park, PA, USA. AAI3343661.

Chen, Yuguo, Diaconis, Persi, Holmes, Susan P., & Liu, Jun S. (2005). Sequential Monte Carlo Methods for Statistical Analysis of Tables. *Journal of the american statistical association*, **100**(469), 109–120.

Comin, Cesar H., Silva, Filipi N., & da F. Costa, Luciano. (2014). *A framework for evaluating complex networks measurements*.

Cozzo, Emanuele, Kivel, Mikko, Domenico, Manlio De, Sol, Albert, Arenas, Alex, Gmez, Sergio, Porter, Mason A., & Moreno, Yamir. (2013). *Structure of triadic relations in multiplex networks*.

Csardi, Gabor, & Nepusz, Tamas. (2006). The igraph software package for complex network research. *Interjournal, Complex Systems*, 1695.

David, Easley, & Jon, Kleinberg. (2010). *Networks, crowds, and markets: Reasoning about a highly connected world*. New York, NY, USA: Cambridge University Press.

Davis, Allison, Gardner, Burleigh B., & Gardner, Mary R. (1941). *Deep south; a social anthropological study of caste and class*. Chicago: The University of Chicago Press.

Davis, James A. (1967). Clustering and structural balance in graphs. *Human relations*, **20**, 181–187.

Davis, James A. (1970). Clustering and hierarchy in interpersonal relations: Testing two graph theoretical models on 742 sociomatrices. *American sociological review*, **35**(5).

de Sola Pool, Ithiel, & Kochen, Manfred. (1978). Contacts and influence. *Socnet*, **1**(1), 5–51.

Dorogovtsev, Serguei N., Goltsev, Alexander V., & Mendes, José F. F. (2002). Pseudofractal scale-free web. *Phys. rev. e*, **65**, 066122.

Doroud, Mina, Bhattacharyya, Prantik, Wu, Shyhtsun Felix, & Felmlee, Diane. (2011). The evolution of ego-centric triads: A microscopic approach toward predicting macroscopic network properties. *Pages 172–179 of: Socialcom/passat*. IEEE.

Faust, Katherine. (1997). Centrality in affiliation networks. *Social networks*, **19**(2), 157–191.

Faust, Katherine. (2008). Triadic configurations in limited choice sociometric networks: Empirical and theoretical results. *Social networks*, **30**(4), 273–282.

Freeman, Linton C. (1992). The sociological concept of "group": An empirical test of two models. *The american journal of sociology*, **98**(1), 152–166.

Freeman, Linton C. (2003). Finding social groups: A meta-analysis of the southern women data. *Pages 39–97 of: Dynamic social network modeling and analysis*. the national academies. Press.

Galaskiewicz, Joseph. (1985). *Social organization of an urban grants economy: A study of business philanthropy and non-profit organizations*. Academic Press.

Glänzel, Wolfgang, & Schubert, András. (2004). *Analyzing scientific networks through co-authorship*. Open Access publications from Katholieke Universiteit Leuven. Katholieke Universiteit Leuven.

Granovetter, Mark S. (1973). The Strength of Weak Ties. *The american journal of sociology*, **78**(6), 1360–1380.

Gupte, Mangesh, & Eliassi-Rad, Tina. (2012). Measuring tie strength in implicit social networks. *Pages 109–118 of: Contractor, Noshir S., Uzzi, Brian, Macy, Michael W., & Nejdl, Wolfgang (eds), WebSci*. ACM.

Harary, Frank, & Komrel, Helene J. (1979). Matrix measures for transitivity and balance. *J. Math. Sociol.*, **6**, 199–210.

Hell, Pavol. (1979). An introduction to the category of graphs. *Pages 120–136 of: Topics in graph theory* (New York, 1977). Ann. New York Acad. Sci., vol. 328. New York Acad. Sci., New York.

Holland, Paul W., & Leinhardt, Samuel. (1971). Transitivity in structural models of small groups. *Small group research*, **2**, 107–124.

Juszczyzyn, Krzysztof, Budka, Marcin, & Musial, Katarzyna. (2011). The dynamic structural patterns of social networks based on triad transitions. *Pages 581–586 of: Asonam*. IEEE Computer Society.

Kimberlin, Carole L., & Winterstein, Almut G. (2008). Validity and reliability of measurement instruments used in research. *Am j health syst pharm*, **65**(23), 2276–2284.

Kreher, Donald L., & Stinson, Douglas Robert. (1999). *Combinatorial algorithms: generation, enumeration, and search*. CRC Press.

Lee, Conrad, & Cunningham, Pádraig. (2013). Community detection: effective evaluation on large social networks. *Journal of complex networks*, Oct.

Liebig, Jessica, & Rao, Asha. (2014). Identifying influential nodes in bipartite networks using the clustering coefficient. *Pages 323–330 of: Proceedings of the tenth international conference on signal-image technology and internet-based systems*.

Martin, Travis, Ball, Brian, Karrer, Brian, & Newman, Mark E. J. (2013). Coauthorship and citation patterns in the physical review. *Phys. rev. e*, **88**(Jul), 012814.

Mitchell, Barry. (1965). *Theory of categories*. Pure and Applied Mathematics. Elsevier Science.

Newman, Mark E. J. (2001). Scientific collaboration networks. I. Network construction and fundamental results. *Phys. rev. e*, **64**(016131).

Newman, Mark E. J. (2003). The structure and function of complex networks. *Siam rev.*, **45**(2), 167–256 (electronic).

Newman, Mark E. J., Strogatz, Steven H., & Watts, Duncan J. (2001). Random graphs with arbitrary degree distributions and their applications. *Phys. rev. e*, **64**(Jul), 026118.

Opsahl, Tore. (2013). Triadic closure in two-mode networks: Redefining the global and local clustering coefficients. *Social networks*, **35**(2), 159 – 167. Special Issue on Advances in Two-mode Social Networks.

R Development Core Team. (2008). *R: A language and environment for statistical computing*. R Foundation for Statistical Computing, Vienna, Austria. ISBN 3-900051-07-0.

Ravasz, Erzsébet, Somera, Anna Lisa, Mongru, Dale A., Oltvai, Zoltán N., & Barabási, Albert-László. (2002). Hierarchical organization of modularity in metabolic networks. *Science*, **297**(5586), 1551.

Saramäki, Jari, Kivelä, Mikko, Onnela, Jukka-Pekka, Kaski, Kimmo, & Kertész, János. (2007). Generalizations of the clustering coefficient to weighted complex networks. *Phys. rev. e*, **75**(Feb), 027105.

Scholtens, Denise. *Snadata: Social networks analysis data examples*. R package version 1.10.0.

Slater, Noa, Itzchack, Royi, & Louzoun, Yoram. (2014). Mid size cliques are more common in real world networks than triangles. *Network science*, **2**(12), 387–402.

Stanley, Richard P. (2002). *Enumerative combinatorics*. Cambridge studies in advanced mathematics, no. v. 1. Cambridge University Press.

Szabó, G, Alava, M, & Kertész, J. (2003). Structural transitions in scale-free networks. *Phys rev e*, **67**(5), 056102.

Uzzi, Brian, & Spiro, Jarett. (2005). Collaboration and creativity: The small world problem. *American journal of sociology*, **111**(2), 447–504.

Vázquez, Alexei. (2003). Growing network with local rules: Preferential attachment, clustering hierarchy, and degree correlations. *Phys. rev. e*, **67**(May), 056104.

Wasserman, Stanley, & Faust, Katherine. (1994). *Social network analysis: Methods and applications*. Vol. 8. Cambridge university press.

Watts, Duncan J., & Strogatz, Steven H. (1998). Collective dynamics of “small-world” networks. *Nature*, **393**(6684), 440–442.

Wickham, Hadley. (2009). *ggplot2: elegant graphics for data analysis*. Springer New York.

## A Supplement

Figs. A 1–A 4 elaborate upon the scores in Table 3. Table A 1 is the counterpart, for GWF, to Table 4 in the main text. Fig. A 8 is the counterpart, for DDGGS1 and GWF, of Fig. 9 in the main text, except that the ordered pair for every actor is plotted, rather than their wedge-dependent averages. Fig. A 9 is the counterpart, for DDGGS1, to Fig. 10 in the main text.

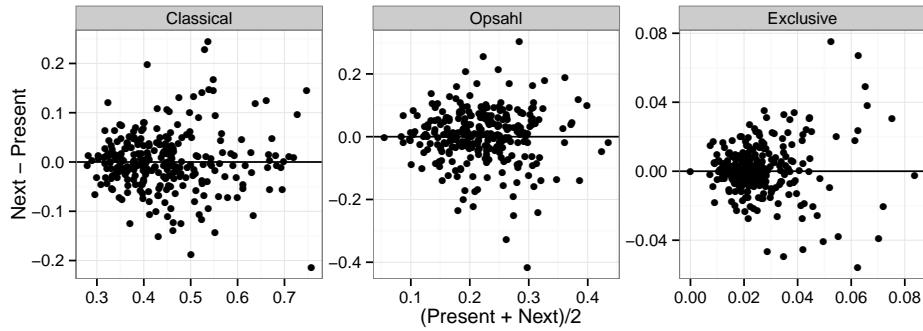


Fig. A 1: Mean–difference plots for values of  $C$ ,  $C^*$ , and  $C^\circ$ , taken across 39 subnetworks of MR over 7 pairs of adjacent intervals.

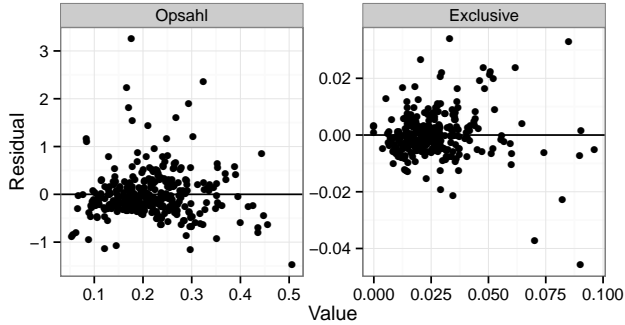


Fig. A 2: Residual plots for  $C/C_{\text{rand}}$  regressed on  $C^*$  and  $D$  regressed on  $C^\circ$ , taken across 39 subnetworks of MR over 8 intervals.

Fig. A 5 depicts histograms of  $C$ ,  $C^*$ , and  $C^\circ$ , evaluated globally on a random sample of 1000 ANs each having the same actor and event degrees as DDGGS1 and GWF. (The samples were performed using the `networksis` package (Admiraal & Handcock, 2008); the samples are not perfectly uniform, so a corrective weighting is applied to the histograms.) Figs. A 6 and A 7 depict analogous histograms for local values of the statistics in each network. In these two figures, the histograms for actors having the same degree (i.e., who attend the same number of events) derive from identical probability distributions.

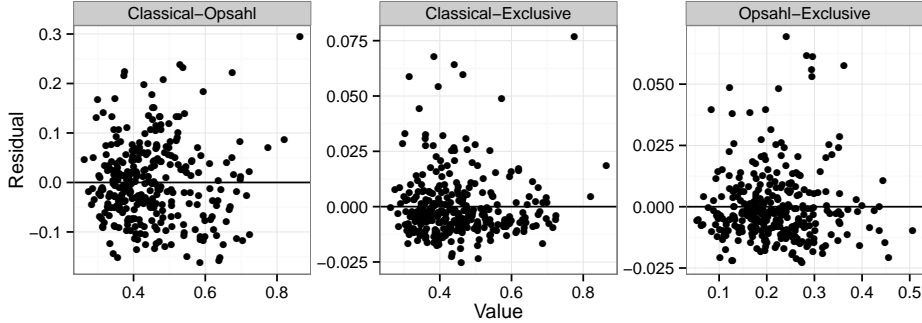


Fig. A 3: Residual plots for  $C^*$  regressed on  $C$ ,  $C^\circ$  regressed on  $C$ , and  $C^\circ$  regressed on  $C^*$ , taken across 39 subnetworks of MR over 8 intervals.

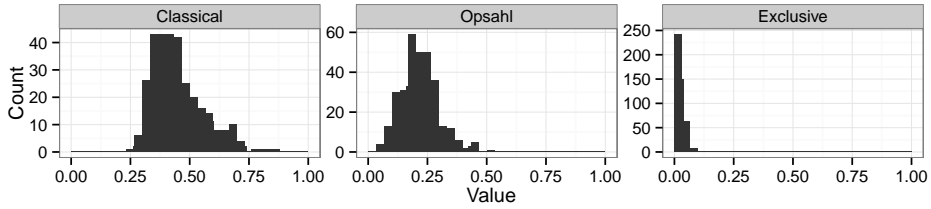


Fig. A 4: Histograms of values of  $C$ ,  $C^*$ , and  $C^\circ$ , taken across 39 subnetworks of MR over 8 intervals.

One stark observation is that the range of values taken across the sample depends greatly on the statistic: Values of  $C$  congregate between .8 and 1. The values of  $C^*$  not only show greater spread for single actors; these spreads are centered over a wider range within  $[0, 1]$ . This is dramatically more so for  $C^\circ$ , especially in the case of actors. This might be seen to support the discriminability of  $C^\circ$  over that of  $C$  and  $C^*$  (see Sec. 3.1). However, the samples are performed in such a way as to control for the influence of repeated events, to

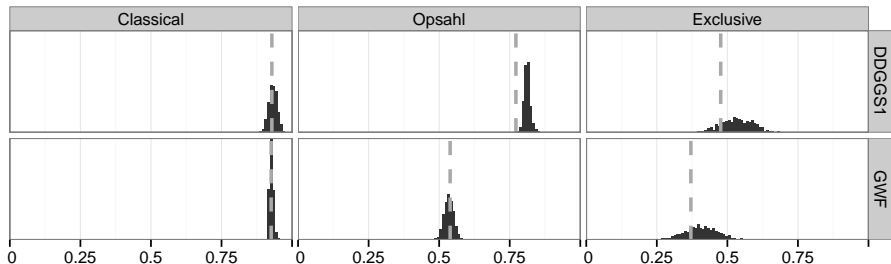


Fig. A 5: Weighted histograms (on a common vertical scale) for  $C$ ,  $C^*$ , and  $C^\circ$  evaluated on null models for DDGGS1 and GWF. Observed values superimposed as dashed lines.

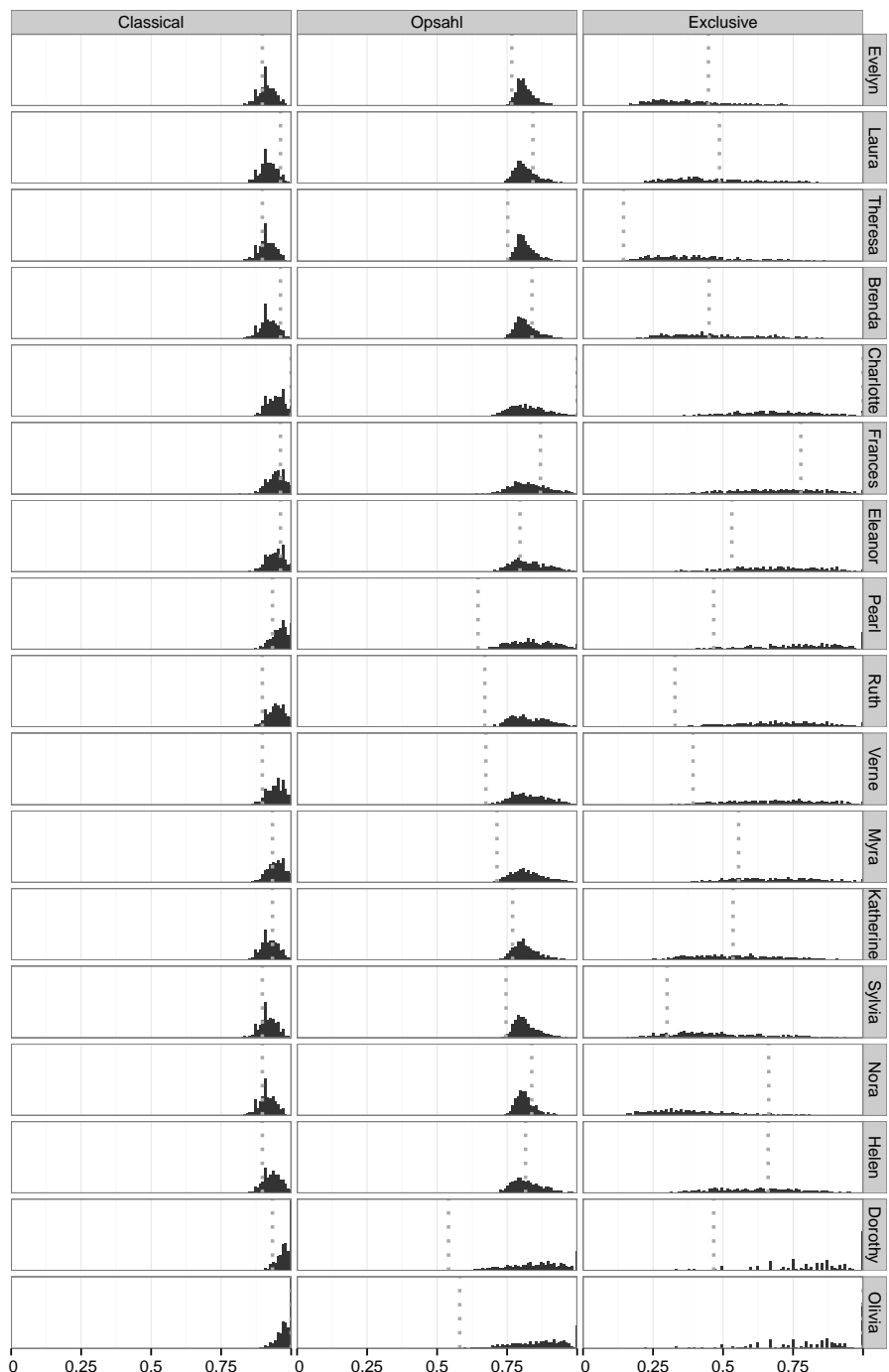


Fig. A 6: Weighted null histograms and observed values of  $C$ ,  $C^*$ , and  $C^\circ$  for the actors of DDGGS1.

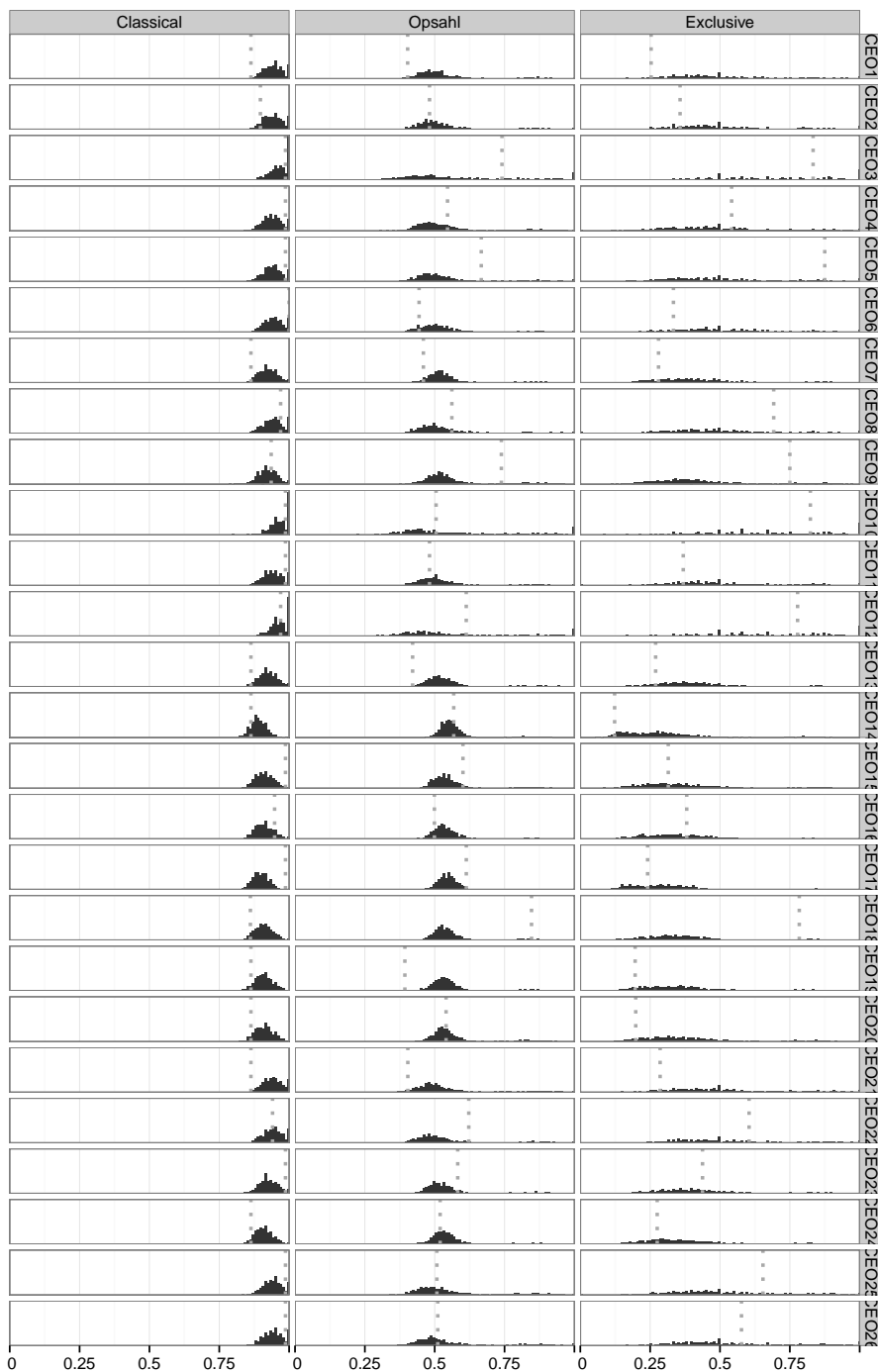


Fig. A 7: Weighted null histograms and observed values of  $C$ ,  $C^*$ , and  $C^\circ$  for the actors of GWF.

Table A 1: Measures of local triadic closure and centrality in GWF.

	Classical	Opsahl	Exclusive	TwoPath	Eigenvector	FourPathCorrected
CEO1	0.863	0.403	0.254	0.192	0.178	-0.010
CEO2	0.897	0.481	0.357	0.139	0.127	-0.007
CEO3	0.987	0.741	0.833	0.130	0.128	-0.001
CEO4	0.987	0.546	0.542	0.202	0.213	0.007
CEO5	0.987	0.667	0.875	0.144	0.140	-0.002
CEO6	1.000	0.444	0.333	0.173	0.174	0.001
CEO7	0.863	0.460	0.280	0.197	0.187	-0.007
CEO8	0.970	0.561	0.692	0.091	0.069	-0.014
CEO9	0.936	0.739	0.750	0.106	0.086	-0.013
CEO10	0.987	0.505	0.824	0.135	0.127	-0.005
CEO11	0.987	0.481	0.368	0.188	0.187	-0.000
CEO12	0.970	0.613	0.778	0.077	0.061	-0.010
CEO13	0.863	0.421	0.270	0.207	0.192	-0.010
CEO14	0.863	0.568	0.123	0.327	0.341	0.008
CEO15	0.987	0.601	0.315	0.245	0.261	0.010
CEO16	0.948	0.499	0.381	0.212	0.211	0.000
CEO17	0.987	0.613	0.241	0.260	0.278	0.012
CEO18	0.861	0.847	0.784	0.178	0.178	-0.000
CEO19	0.863	0.393	0.196	0.226	0.201	-0.016
CEO20	0.863	0.541	0.198	0.279	0.289	0.006
CEO21	0.863	0.404	0.286	0.183	0.168	-0.009
CEO22	0.941	0.622	0.604	0.168	0.168	0.000
CEO23	0.987	0.582	0.438	0.221	0.235	0.009
CEO24	0.863	0.519	0.275	0.240	0.239	-0.002
CEO25	0.987	0.508	0.654	0.183	0.188	0.004
CEO26	0.987	0.511	0.577	0.183	0.188	0.004

which all three statistics are sensitive, but to preserve the influence of event size, to which only  $C$  and  $C^*$  are sensitive (see Sec. 1.2); that is, the sampling method itself confers a discriminability advantage unto  $C^\circ$ .

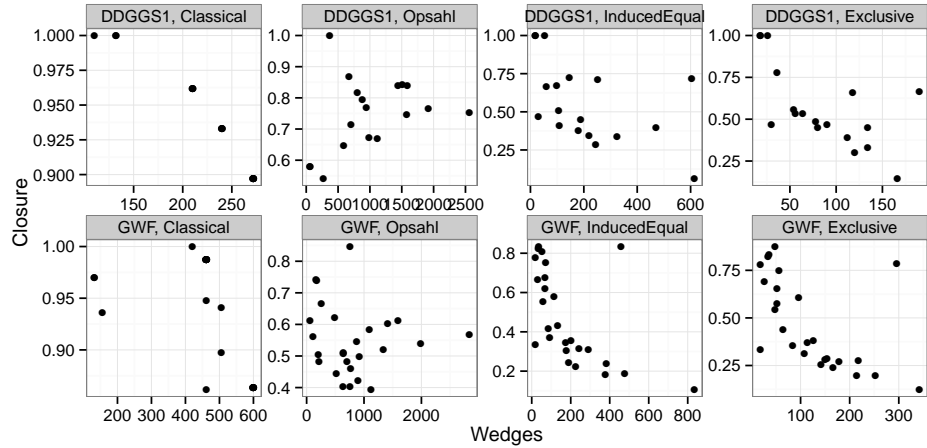


Fig. A 8: Four wedge-dependent local clustering coefficients in DDGGS1 and GWF.

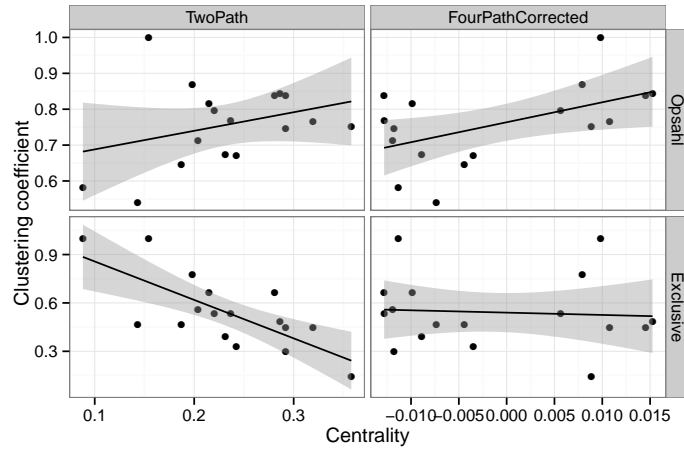


Fig. A 9: Scatterplots of Opsahl and exclusive clustering coefficients versus 2-path and 4-path-corrected eigenvector centrality scores across actors in DDGGS1. Least-squares regression lines and 95% confidence bands are overlaid.